Nonadiabatic bulk-surface oscillations in driven topological insulators

Michael Kolodrubetz, Benjamin M. Fregoso, and Joel E. Moore

Non-adiabatic bulk-surface oscillations in driven topological insulators

Michael Kolodrubetz,[1, 2] Benjamin M. Fregoso,[1] and Joel E. Moore[1, 2]

[1]*Department of Physics, University of California, Berkeley, California, 94720, USA*
[2]*Materials Sciences Division, Lawrence Berkeley National Laboratory, Berkeley, California 94720, USA*

Recent theoretical and experimental work has suggested the tantalizing possibility of opening a topological gap upon driving the surface states of a three-dimensional strong topological insulator (TI) with circularly polarized light. With this motivation, we study the response of TIs to a driving field that couples to states near the surface. We unexpectedly find coherent oscillations between the surface and the bulk and trace their appearance to unavoidable resonances caused by photon absorption from the drive. We show how these resonant oscillations may be captured by the Demkov-Osherov model of multi-level Landau-Zener physics, leading to non-trivial consequences such as the loss of adiabaticity upon slow ramping of the amplitude. We numerically demonstrate that these oscillations are observable in the time-dependent Wigner distribution, which is directly measurable in time-resolved ARPES experiments. Our results apply generically to any system with surface states in the presence of a gapped bulk, and thus suggest experimental signatures of a novel surface-bulk coupling mechanism that is fundamental for proposals to engineer non-trivial states by periodic driving.

The recent emergence of topological physics in bulk materials has brought to bear an important connection between topology in the bulk and novel surface states. These surface states manifest a variety of interesting properties, such as exhibiting anomalous behavior that is impossible in a purely two-dimensional theory. The simplest example of this is the one-dimensional chiral edge states in the quantum Hall effect[1–4], and the same concept applies to helical surface states and isolated Dirac cones in two- and three-dimensional topological insulators respectively[5–11], as well as more exotic cases like Fermi arcs in Weyl and Dirac semimetals[12–17]. Indeed, an ever-expanding zoo of surface states is continuously being discovered[18–29].

These surface states are particularly amenable to detection by a host of modern experimental methods, such as scanning tunneling microscopy (STM)[30–35] and angle-resolved photoemission spectroscopy (ARPES)[11,15–17,26]. These probes preferentially excite electrons near the surface and are thus able to measure and distinguish surface and bulk states. A more recent development in ARPES as well as similar photon-in photon-out experimental setups is time-resolved pump-probe spectroscopy, in which the system is be excited far from equilibrium and the state detected during the relaxation process[36–44]. This gives much richer insight into both the static and dynamic properties of the quantum system and has also given rise to a recent re-emergence of theory for such far-from-equilibrium systems. In particular, there is an active search for examples of drive-induced topological phases[45–47] and significant theoretical progress towards their classification[48–53].

One important development in the field has been a recent experiment[41] in which a time-reversal-invariant topological insulator (TI) was irradiated with a pulse of light and imaged via pump-probe ARPES. The Dirac cone on the surface of these materials is a seed of new topological physics, and the experiment sees a gap open in the Dirac cone upon applying circularly polarized light.

This gap is predicted to be topological in the sense that it realizes a half-integer quantum Hall effect.[54,55]

Motivated by this development, in this paper we explore the non-equilibrium dynamics of a topological insulator in the presence of a short pulsed drive. The pulse breaks the perfect periodicity of the drive, yet we numerically see Floquet-Bloch sidebands as in the experiments. However, we find an unexpected oscillation in the intensity of these sidebands, which we identify as a novel bulk-surface coupling induced by the local drive at the surface. We show that this coupling leads to *coherent* oscillations between the surface and the bulk that survive in the thermodynamic limit, which generically arise through a simple many-level Landau-Zener picture that depends on Floquet resonances. This model yields several non-trivial predictions, including reversing the meaning of adiabaticity its traditional non-resonant behavior: faster ramps appear more "adiabatic" because they see the resonances for less time, and thus decreasing the ramp rate leads to stronger bulk-surface oscillations. We find that these resonant oscillations are not only visible in the Wigner distribution, a non-equilibrium observable measurable in pump-probe ARPES, but are completely generic to periodically-driving the surface of any material with surface states inside a gapped bulk. This provides a measurable signature of this non-trivial surface-bulk resonance that should play a major role in Floquet engineering of driven surface states.

The paper is organized as follows. In Section I we introduce the idea of Floquet-Bloch states and a non-equilibrium observable – the Wigner distribution – that can be used to measure them. We then discuss the behavior of these states at constant amplitude of drive for the simplest single-Dirac-cone model of TI surface states followed by a more complicated model in which coupling is allowed to the bulk. In Section II we see how the Floquet-Bloch states are modified by turning the drive on and off non-adiabatically via a Gaussian pump pulse. One important effect that we see is resonance between
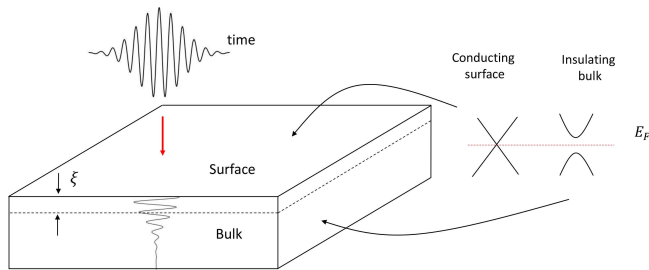
FIG. 1. Illustration of the setup that we consider. A pulsed periodic electric field is incident on the surface of a topological insulator and decays with some characteristic length scale ξ into the bulk. Also shown the band structure of a topological insulator (TI). The bulk appears to be a gapped semiconductor, but the difference in the topological $\mathbb{Z}_2$ invariant between the TI and the surrounding vacuum leads to Dirac cone surface states.

the surface and bulk, which we proceed to describe using a many-level generalization of Landau-Zener tunneling known as the Demkov-Osherov model. Finally, in Sec. III, we analytically derive other leading corrections to the adiabatic Floquet-Bloch signal using the Floquet generalization of adiabatic perturbation theory.

I. FLOQUET-BLOCH STATES FOR CONSTANT AMPLITUDE DRIVE

A schematic setup used in many contemporary condensed matter experiments is illustrated in Fig. 1. A laser pulse illuminates the sample, driving the electrons out of equilibrium. The non-equilibrium electrons are then measured via one of a number of methods, e.g., optical response, photoemission, tunneling, etc. This type of setup is particularly interesting in the case of topological insulators, whose surface states may be readily excited by the drive. In addition, as the bulk states have some (weak) overlap with the drive, they also are excited. This is precisely the effect that is used in pump-probe experiments of high-temperature superconductors and other materials, where the non-equilibrium (bulk) population in excited states is seen to decay as a probe of the material's physics.

We will examine the response of topological insulators to this type of drive. These materials have a gapped bulk and conducting Dirac-like surface states, as illustrated in Fig. 1. The surface states have been probed through a number of techniques including pump-probe ARPES. However, due to their gapped nature, understanding the connection between the surface and the bulk states has remained relatively unexplored area. In this paper we will show that an interesting connection exists and discuss its observable consequences.

A. Driving surface states of TIs

The simplest model of a TI surface state is a single Dirac cone with Hamiltonian[9]

$$H_{\text{SS}} = -v(k_x \sigma^x + k_y \sigma^y), \tag{1}$$

for a surface perpendicular to $\hat{z}$. The Pauli matrices often correspond to physical spin $(S^x, S^y) = (\sigma^y, -\sigma^x)/2$ which is locked perpendicular to the momentum $\mathbf{k}_\parallel$ via Rashba spin-orbit coupling[56–58], though more generally σ could denote spin/orbital indices. Our units are set by velocity $v = 1$, as well as $\hbar = 1$ throughout the paper. Consider driving this Hamiltonian by a laser perpendicular to the surface, with electric field $\mathbf{E} = E_x \cos(\Omega t + \varphi_x)\hat{x} + E_y \sin(\Omega t + \varphi_y)\hat{y}$ of constant amplitude. This drive allows arbitrary polarization, but we will focus on the case of linearly y-polarized light and phase $\varphi_y = 0$. Coupling this periodic drive to the surface states is achieved by the minimal substitution $\mathbf{k}_\parallel \to \mathbf{k}_\parallel - e\mathbf{A}$, where we pick the gauge $\mathbf{E} = -\partial \mathbf{A}/\partial t$. Then the Hamiltonian becomes time-dependent:

$$H(t) = H_{\text{SS}}(\mathbf{k}_\parallel - e\mathbf{A}(t)) . \tag{2}$$

We first consider the case of constant drive amplitude, $E_y = \Omega A_y$, but later we will return to the case where this amplitude in turn varies slowly as in the case of a pulsed laser (cf. Fig. 2b). Note that we are assuming the drive is uniform over the entire sample such that the in-plane momentum $\mathbf{k}_\parallel$ remains a conserved quantity even in the presence of the drive.

1. Non-equilibrium observables: Wigner distribution and Floquet-Bloch states

Acting on the Hamiltonian in Eq. 1 with a periodic drive yields a fundamentally non-equilibrium problem. Floquet's theorem states that the full time evolution $U(t) = \mathcal{T} \exp[-i \int H(t)dt]$ ($\mathcal{T}$ = time ordering) can be decomposed as

$$U_{\mathbf{k}\parallel}(t) = P_{\mathbf{k}\parallel}(t)e^{-iH_F(\mathbf{k}\parallel)t}, \tag{3}$$

where $P_{\mathbf{k}\parallel}(0) = \mathbb{1}$ and $P_{\mathbf{k}\parallel}(t) = P_{\mathbf{k}\parallel}(t + 2\pi/\Omega)$. P is a periodic operator often called the micromotion and $H_F^{k\parallel}$ is an effective static Hamiltonian - the Floquet Hamiltonian - that describes the behavior over many cycles. This is the temporal analogue of Bloch's theorem, in addition to which we have used the usual Bloch's theorem in noting that $\mathbf{k}_\parallel$ is conserved. The eigenstates of $H_F^{k\parallel}$ satisfying $H_F(\mathbf{k}_\parallel)|n_F(\mathbf{k}_\parallel)\rangle = \epsilon_F^n(\mathbf{k}_\parallel)|n_F(\mathbf{k}_\parallel)\rangle$ are known as Floquet-Bloch states[41,59,60]. A system prepared in one of these Floquet-Bloch states at time $t = 0$ will return to the same state stroboscopically at times $t = nT$ for integer n, where $T = 2\pi/\Omega$ is the driving period.

For such a non-equilibrium system, one of the most natural observables to consider is the probability to be in

each of the Floquet-Bloch eigenstates. This is naturally described by the non-equilibrium generalization of the occupation number, namely the Wigner distribution:

$$f_{\alpha\beta}(\mathbf{k}_\parallel, \omega, t_{\text{av}}) = -iG^<_{\alpha\beta}(\mathbf{k}_\parallel, \omega, t_{\text{av}})$$
$$= -i\mathcal{F}_{t_r}\left[\langle c^\dagger_\beta(t_{\text{av}} + t_r/2)c_\alpha(t_{\text{av}} - t_r/2)\rangle\right],$$

where α and β denote spin/orbital indices and $\mathcal{F}$ is the Fourier transform. To ensure basis-independence we will be interested in its trace, $f(\mathbf{k}_\parallel, \omega, t_{\text{av}}) \equiv \sum_\alpha f_{\alpha\alpha}(\mathbf{k}_\parallel, \omega, t_{\text{av}})$.

The Wigner distribution naturally describes equilibrium or non-equilibrium occupation of energy eigenstates[61]. The simplest example of this is to consider evolution of the state $|\psi\rangle = c^\dagger_0|vac\rangle$ under a static single-particle Hamiltonian, where $c^\dagger_0$ creates a single fermion in the energy eigenvalue E_0 of H. Then a straightforward calculation confirms that f is just a single peak at frequency E_0:

$$f(t_r, t_{\text{av}}) = \langle\psi|\sum_n c^\dagger_n(t_{\text{av}} + t_r/2)c_n(t_{\text{av}} - t_r/2)|\psi\rangle$$
$$= \sum_n \langle\psi|\left(e^{iH(t_{\text{av}}+t_r/2)}c^\dagger_n e^{-iH(t_{\text{av}}+t_r/2)}\right.$$
$$\left. e^{iH(t_{\text{av}}-t_r/2)}c_n e^{-iH(t_{\text{av}}-t_r/2)}\right)|\psi\rangle$$
$$= e^{iE_\psi t_r}\sum_n \langle\psi|c^\dagger_n e^{-iHt_r}c_n|\psi\rangle = e^{iE_0 t_r}$$
$$f(\omega, t_{\text{av}}) = 2\pi\delta(\omega - E_0). \tag{4}$$

Similarly, if we start with many electrons, $|\psi\rangle = c^\dagger_0\cdots c^\dagger_{N-1}|vac\rangle$, then a similar calculation shows that f is just a sum of peaks at each electron's energy: $f(\omega) = 2\pi\sum_{j=0}^{N-1}\delta(\omega - E_j)$. Thus the Wigner distribution gives information about not only the occupation via the amplitude of the delta-function peaks (2π per electron), but also about their time-evolution via the peak frequency.

These ideas are particularly useful in driven Floquet systems as they are out-of-equilibrium from the get go. Before deriving the Wigner distribution of a system in a Floquet eigenstate, let's start by considering the more generic case where one starts in an eigenstate of some static H at time t_0 but then turns on an arbitrary driving $H(t)$. As long as the Hamiltonian remains non-interacting, by Wick's theorem the Wigner distribution will remain the sum over occupied eigenstates of the single-particle f. So if we start from some single-particle state $|\psi_n(t_0)\rangle \equiv c^\dagger_n|vac\rangle$ and then turn on arbitrary drive, it is readily confirmed that f is simply given by

$$f_n(t_r, t_{\text{av}}) = \langle\psi_n(t_{\text{av}} + t_r/2)|\psi_n(t_{\text{av}} - t_r/2)\rangle, \tag{5}$$

where $|\psi_n(t)\rangle = U(t, t_0)|\psi_n(t_0)\rangle$ is the state obtained by full time evolution starting from $|\psi_n(t_0)\rangle$. For N occupied single particle states one simply sums over $n = 0, 1, \ldots, N-1$.

Now consider a Floquet-Bloch eigenstate $|n_F(\mathbf{k}_\parallel)\rangle$. As we work with translationally-invariant drives throughout this paper, we will occasionally suppress the $\mathbf{k}_\parallel$ dependence. Associated with a given Floquet eigenstate are a time-periodic family of wave functions,

$$|n_F(t)\rangle \equiv P(t)|n_F\rangle, \tag{6}$$

which describe how $|n_F\rangle$ evolves during a cycle. Note that by our convention for P, $|n_F(0)\rangle = |n_F\rangle$. As this state is periodic, we may Fourier decompose it:

$$|n_F(t)\rangle = \sum_\ell e^{i\ell\Omega t}|n_F^{(\ell)}\rangle. \tag{7}$$

These Floquet modes $|n_F^{(\ell)}\rangle$ play an important role in the theory. In particular, if we plug the Floquet eigenstate into Eq. 5, we see that

$$f_n(t_r, t_{\text{av}}) = \langle\psi_n(t_{\text{av}} + t_r/2)|\psi_n(t_{\text{av}} - t_r/2)\rangle$$
$$= \sum_{\ell\ell'} e^{i(\ell-\ell')\Omega t_{\text{av}}}e^{i[\epsilon_F^n - (\ell+\ell')\Omega/2]t_r}\langle n_F^{(\ell')}|n_F^{(\ell)}\rangle,$$

where $|\psi_n(t)\rangle = e^{-i\epsilon_F^n t}|n_F(t)\rangle$ accounts for time evolution due to both micromotion and the Floquet Hamiltonian (see Eq. 3). This expression simplifies even further in an important limit, namely when we average over the "measurement time" t_{av}. This naturally emerges in a number of physically-relevant situations. For instance, if we put back in the phase of the drive, which enters the previous expression as $\Omega t_{\text{av}} \to \Omega t_{\text{av}} + \varphi$, then averaging over the often experimentally-uncontrolled phase is equivalent to averaging over t_{av}. Equivalently, one often finds that there is experimental imprecision on the time of measurement and/or the relative phase of the pump and the probe. If this imprecision is long compared to the drive period, again the averaging emerges. Denoting this so-called Floquet non-stroboscopic (FNS[62]) averaging by an overline, we see that[63,64]

$$\overline{f_n(t_r)} = \sum_\ell e^{i(\epsilon_F^n - \ell\Omega)t_r}\langle n_F^{(\ell)}|n_F^{(\ell)}\rangle$$
$$\overline{f_n(\omega)} = 2\pi\sum_\ell \delta(\omega - \epsilon_F^n + \ell\Omega)\langle n_F^{(\ell)}|n_F^{(\ell)}\rangle.$$

So each electron state is "split" into Fourier modes at frequency $\epsilon_F^n - \ell\Omega$ with amplitude $p_{n\ell} = \langle n_F^{(\ell)}|n_F^{(\ell)}\rangle$. Note that these peaks sum up to 1 total electron, $\sum_\ell p_{n\ell} = 1$, by the normalization of $|n_F\rangle$. So we see that the Wigner distribution again provides insight on the frequency of these sidebands as well as the probability to occupy them.

Let us now apply these ideas to driving the surface states of the TI, described by the Hamiltonian in Eq. 1. As we have shown, the signal at each $\mathbf{k}_\parallel$ is just the sum over the signals from each of the occupied states. In Fig. 2a we plot the Wigner distribution in the Floquet eigenstates with both branches of the Dirac cone occupied for distinct (but constant in time) drive amplitude. For the remainder of the paper, we focus on linearly-polarized
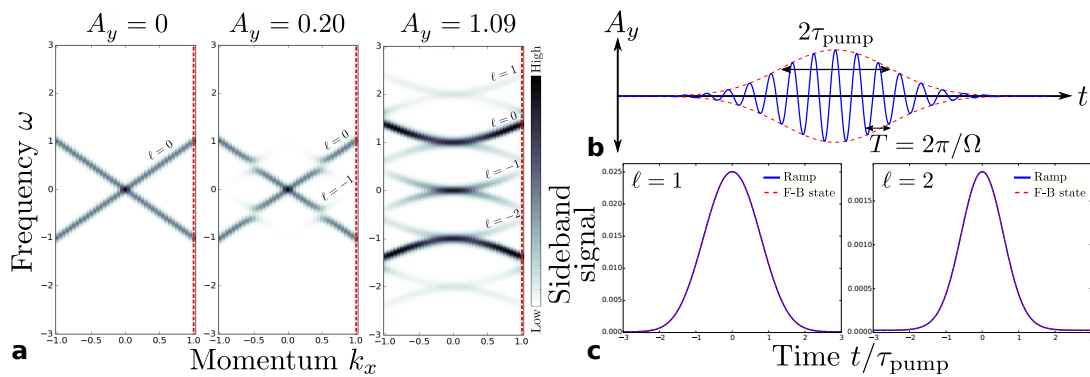
FIG. 2. Driving Dirac surface states of a TI model (Eq. 1) without any bulk states. (a) Wigner distribution of "equilibrium" Floquet-Bloch states with varying drive strength A_y, as derived in Eq. 8, showing hybridization of the surface states. The chemical potential $\mu > 0$ is chosen such that both surface states are occupied. Delta-function peaks corresponding to Floquet-Bloch states have been broadened by a Gaussian of width $\tau_{\text{pr}} = 24$ for clarity. (b) Illustration of the pulsed drive that we will consider. For the driven Dirac model, both states in the Hilbert space are occupied, so in the slow-ramp limit ($\tau_{\text{pump}} \gg T$) there are no additional excitations due to the ramp. This is illustrated in (c) by plotting the amplitude in the $\ell = 1, 2$ sidebands for $k_x = 1$, which show no difference between the instantaneous Floquet-Bloch eigenstates (dashed red) and the full time evolution during the ramp (blue). Data is for a linearly-polarized pump perpendicular to the momentum, with parameters $\tau_{\text{pump}} = 60$, $A_y^0 = 1.09$, and $\Omega = 1$.

light whose polarization direction ($\hat{y}$) is orthogonal to the momentum ($k_y = 0$). Other choices of polarization and momentum give qualitatively similar results. As noted in the plots and seen elsewhere[45,47,59,65,66], anti-crossings between the surface states occur open up near the resonance between the branches. This is the first example we will see of Floquet resonance, here between two surface states. These Floquet resonances, and in particular more complicated ones between the surface and the bulk, will play a starring role in the remainder of the paper.

As we will discuss in more detail later, actual experiments involve a pulsed rather than fixed drive, as illustrated in Fig. 2b. In the slow ramp limit, $\tau_{\text{pump}} \gg T$, which we always restrict ourselves to, the drive is approximately periodic at any point in time and we might expect the system to adiabatically follow the instantaneous Floquet-Bloch eigenstates. In general, if we ramp too fast, we expect non-adiabatic effects as we fail to adiabatically follow these eigenstates. However, we note that because both bands are occupied, there are *no* non-adiabatic effects in this purely surface state model no matter how short the pulse. The reason is simply that both states in the two-level system are filled, and there is simply nowhere else in the Hilbert states for the electrons to go. This is seen in Fig. 2c, where the ℓth sidebands of the Wigner distribution of the Floquet-Bloch eigenstates are compared to those of the full time evolution, showing no difference for $\tau_{\text{pump}} \gg T$.

We are primarily interested in non-adiabatic effects in the periodically-driven system due to the pulse. We will show that such novel behavior can occur when coupling these states to an empty bulk conduction band. Therefore, let us now consider the presence of the bulk and see how it affects this story.

B. Driving surface and bulk states of TIs

To understand the relevance of the bulk, we want to start by constructing a simple tight-binding model of a three-dimensional topological insulator. We consider one of the simplest such bulk models[54], namely the lattice regularization of $(\mathbf{k} \cdot \boldsymbol{\sigma})\tau^z + m\tau^x$:

$$H_{\text{bulk TI}} = (\sigma^x \sin k_x + \sigma^y \sin k_y + \sigma^z \sin k_z)\tau^z + (m + 3 - \cos k_x - \cos k_y - \cos k_z)\tau^x, \quad (8)$$

where σ and τ are two sets of Pauli matrices corresponding to, e.g., spin and orbital degrees of freedom. We again assume that the electric field couples via the minimal substitution, but now with the caveat that the electric field strength decays into the bulk with length scale ξ, as in Fig. 1. Choosing the surface of interest to again be perpendicular to $\hat{z}$, $\mathbf{k}_\parallel = (k_x, k_y)$ remain good quantum numbers. For more details of the hopping Hamiltonian in the z-direction, please see Appendix A.

In the absence of drive, this model gives a topological insulator for $-4 < m < 0$ and a trivial insulator otherwise. In the presence of drive, we can solve this Floquet problem and calculate its Wigner distribution. The results are shown in Fig. 3a. Similar to the simple surface-only model, the surface states are strongly dressed by the drive, although details of the signal depend heavily on microscopic details of the model. At strong driving strength $A_y = 0.25$, this "Floquet equilibrium" (i.e., constant drive amplitude) data already shows how coupling to the bulk changes the story, resulting in $\ell = 3$ and 4 sidebands that are stronger than $\ell = 2$ due to resonant surface-bulk hybridization. In the next section we will see that this surface-bulk coupling has a strong effect when we consider a pulsed drive.

II. NON-ADIABATIC EFFECTS OF THE PULSED DRIVE

While the previous section considered the response in Floquet eigenstates, which would come for example from the steady-state of a continuous-wave laser, it is often more experimentally practical to use pulsed sources. This has undesirable effects such as losing perfect periodicity, but the ability to change the pulse length can also be a powerful tool to prevent heating and target a unitary response of the system. Therefore, in this section we will concern ourselves with the question of how finite pulse width affects the non-equilibrium observables of driven topological insulators.

A pulsed laser may be modeled by simply multiplying the periodic drive by a slow envelope, such as a Gaussian: $\mathbf{A}(t) = [A_x^0 \cos(\Omega t)\hat{x} + A_y^0 \sin(\Omega t)\hat{y}] \exp(-t^2/2\tau_{\text{pump}}^2)$.[67] The envelope breaks periodicity and thus renders this no longer an exact Floquet problem, though in the limit of a long pulse it is approximately periodic at any given point in time. One might then expect that the system will adiabatically track the Floquet eigenstates, yielding Wigner distributions similar to Figs. 2a and 3a. This is almost correct but, as we will now see, only part of the story.

A. Coherent bulk-surface oscillations

We now simulate the coupled bulk-surface model of a TI under such pumped drive. We start deep in the past with the drive turned off and the chemical potential set such that all bulk valence band and surface states are occupied.[69] Then the exact dynamics are simulated and the Wigner distribution $f(\omega, t_{\text{av}})$ computed. This function is strongly peaked in ω and highly oscillatory in t_{av} so we smooth out the results by convolving f by a Gaussian of width τ_{pr} in both the frequency and time direction:

$$I(\omega, t_{\text{av}}) = \int d\omega' dt'_{\text{av}} e^{-(\omega-\omega')^2 \tau_{\text{pr}}^2} e^{-(t_{\text{av}}-t'_{\text{av}})^2/\tau_{\text{pr}}^2} f(\omega', t'_{\text{av}}).$$

(9)

We refer to the result as the signal and/or intensity at frequency ω and time t_{av}, which will be justified in Sec. II C by showing its connection to ARPES. If the "probe width" τ_{pr} is much greater than the drive frequency, this convolution has the additional advantage of averaging over the drive phase, such that f may be replaced by $\overline{f}$ in Eq. 9.

One striking difference between the equilibrium and non-equilibrium case is that, even after the drive has been turned off, population remains in the bulk conduction states, as seen in Fig. 3d. This phenomenon is specific to the coupled bulk/surface model, and we do not see it in the simpler Dirac cone model of Sec. I A. Decay of excited surface states into the bulk has been anticipated in the presence of phonons[40], but note that this decay mechanism does not exist in our model. Therefore, the

population transferred to the bulk may only come from coherent non-adiabatic processes.

In addition to tunneling into the bulk, we see coherent oscillations in the Wigner distribution of the surface states. This is shown in Fig. 3b and c, where the signal in the ℓth sideband is given by weight in the ℓth peak at fixed k_x and t_{av} normalized by the sum over all peaks. Together, these results suggest that we are seeing coherent oscillations of the population between the surface and the bulk states. We have varied the microscopic parameters over a wide range of values and found that the existence of these oscillations are remarkably robust, always appearing in tandem with an irreversible "leaking" into the bulk. We now seek to understand this in terms the physics of Floquet resonances.

B. Floquet resonances and Landau-Zener physics

Resonances have long been known to play a major role in Floquet systems[70–73]. Mathematically, they come from the fact that the drive introduces a new energy scale Ω such that energies are only defined modulo Ω. For a many-body system of linear size L in d dimensions, the bare spectrum is extensive, scaling as L^d. However, Hone et al.[73] argued that folding by Ω in the thermodynamic limit leads to a denser and denser set of quasi-energy levels as the system size is increased. This in turn leads to a dense set of weakly-avoided crossings such that even simple ideas like tracking a single quasi-energy level to achieve an adiabatic limit becomes ill-defined. Thus the weakly-avoided crossings, which we call Floquet resonances, lead to a fundamental absence of adiabaticity in Floquet systems. Furthermore, they have been suggested to lead to heating effects[74] and the breakdown of high-frequency expansions[75], which are two of the most important and active topics in the field of Floquet engineering.

As seen in Fig. 3a, Floquet resonances between the surface and the bulk states inevitably occur in systems such as ours, where the driving frequency Ω is less than the bandwidth. However, there are a number of subtleties that we must consider in comparing this to the Hone et al. result. Most notably, they were considering coupling between bulk states due to the drive, whereas here we are interested in coupling between the bulk and the surface state. Since the drive primarily couples to the surface states and only weakly to the bulk, one naive guess would be that the matrix elements between these states would scale as the spatial overlaps between them, ξ/L, vanishing in the thermodynamic limit. This indeed seems to be the case, but one must counterbalance it against the fact that the (one-dimensional) density of states at fixed $\mathbf{k}_\parallel$ scales as L. Thus these two effects conspire to create an order-1 gap in the quasi-energy spectrum which depends sensitively on various microscopic properties. Therefore, we expect that the strength will differ significantly from model to model, e.g., between our simple model TI and
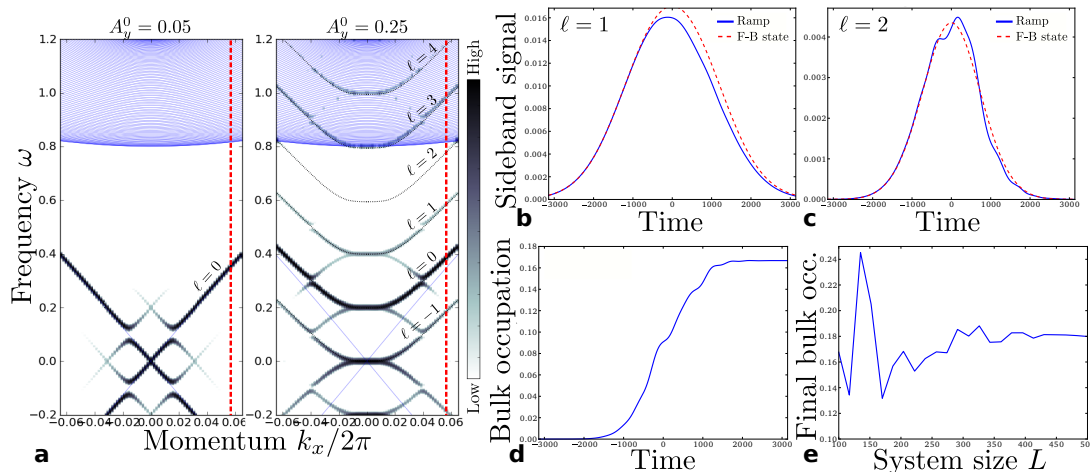
FIG. 3. Driving surface plus bulk states of a model TI (see Eq. 8 and following text). (a) Wigner distribution of Floquet-Bloch eigenstates as a function of driving amplitude. The undriven energy spectrum is shown in blue. The surface states appear similar to Fig. 2a, though in this figure the color plot is on a logarithmic scale to make higher harmonics visible. We also see that starting at approximately $\ell = 3$, the surface-state harmonics appear in the bulk. (b,c) Signal in the $\ell = 1, 2$ surface sidebands for $k_x/2\pi = 0.056$, indicated by the red line in (a). Unlike the driven Dirac model, there is a noticeable difference between the Floquet-Bloch states (dashed red) and the exact time evolution (blue). The intensity in the ℓth harmonic at time t_{av} is given by integrating the signal $I(\omega, t_{av})$ from $\omega = \epsilon_F(\lambda(t_{av})) + (\ell - 1/2)\Omega$ to $\epsilon_F(\lambda(t_{av})) + (\ell + 1/2)\Omega$ while the "equilibrium" value is estimated by manually removing resonances[68]. (d) Signal in the bulk bands as a function of t_{av}, given by integrating the signal for all $\omega > E_{bulk}$. (e) Final probability to occupy the bulk states after the ramp is finished ($t \to \infty$) as a function of system size showing the existence of a well-defined thermodynamic limit. All data are for $k_x/2\pi = 0.056$, $k_y = 0$, $A_x = 0$, $A_y = 0.25$, $m = -0.8$, $\Omega = 0.2$, $\tau_{pr} = 5T = 10\pi/\Omega$, and $L = 100$ unless otherwise specified.

a real material. Nevertheless, the existence of order 1 Floquet resonances should be robust by the above argument, and thus the phenomena we describe are completely generic.

As seen in Fig. 4a, Floquet resonances lead to a series of anti-crossings between quasienergies of the bulk and surface states. As expected, the quasienergy of the surface state depends strongly on driving amplitude, while the bulk states are nearly independent of the drive. We also confirm that as L increases the number of anti-crossings increases as well, while the strength (i.e., the gap) of the anti-crossings decreases. This situation, where a single dispersing level passes through many parallel non-dispersing ones is known in the non-Floquet case as the Demkov-Osherov (D-O) model[76–78], and is an analytically tractable many-level generalization of the Landau-Zener (L-Z) model[79,80]. The scattering matrix of the D-O model in the long-time limit is remarkable because interference between the various avoided crossings is absent. Thus, the D-O scattering problem reduces to N_c independent L-Z transitions, where N_c is the number of bulk levels that the dispersing level surface state crosses. In our case, $N_c \sim L$ at fixed $\mathbf{k}_\parallel$ because we effectively have a one-dimensional problem.

For slow ramps, one expects that the dynamics of a Floquet system will be dominated by resonant effects, which are captured within the appropriately-folded effective Hamiltonian H_F. Therefore, we should be able to able to treat the Floquet D-O model identically to the undriven case. Assume the surface state is ramped through
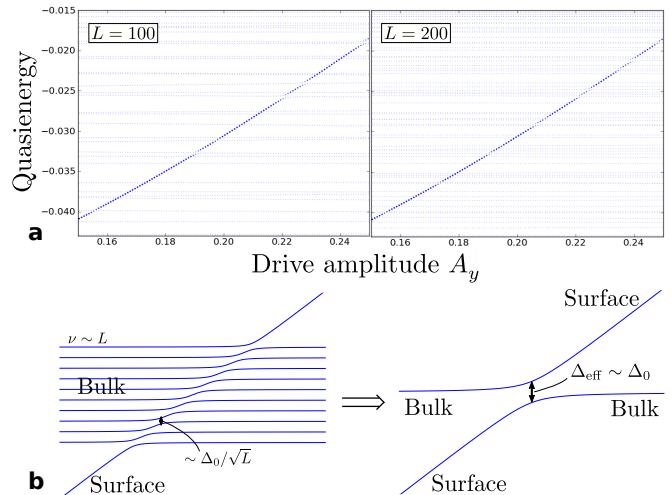

FIG. 4. Floquet resonances between the surface and bulk. (a) Floquet eigenspectrum of the TI model as a function of drive strength using the same parameters as Fig. 3b with $L = 100$ and 200. The size of the dots is proportional to the proximity of the Floquet eigenstate to the top surface such that the surface state appears larger than the bulk states. (b) Illustration of the Demkov-Osherov model of the Floquet eigenspectrum. A single surface state passes through a continuum of bulk states. As L increases, the increase in the density of states is offset by the decrease in the matrix elements coupling surface and bulk. The system may be approximated by a single Landau-Zener crossing with effective gap Δ_{eff} that controls both excitation of the bulk and oscillation frequency of the surface state. See text for details.
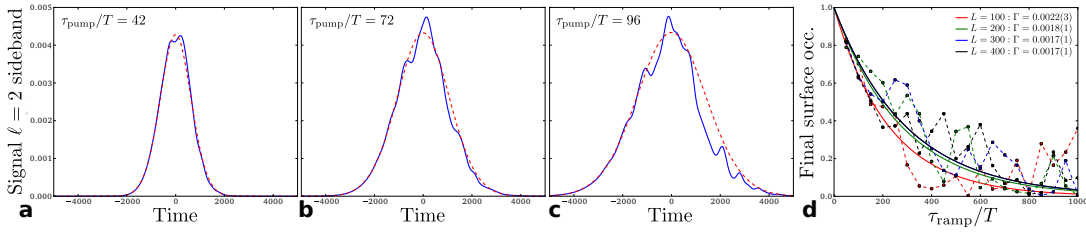
FIG. 5. Scaling of surface oscillations and bulk occupation with pump time τ_{pump}, confirming predictions of the Demkov-Osherov model. (a-c) Oscillations of the signal in the $\ell = 2$ surface sideband as a function of τ_{pump}, showing an increase in amplitude but no apparent change in the characteristic frequency. (d) Final occupation in the surface state, which decreases exponentially with τ_{pump} as the electrons resonantly tunnel into the bulk (see details). The decay rate into the bulk does not depend on system size. All data are for the same parameters as Fig. 3b.

N_c bulk states during the first half of the pump pulse by increasing A_y from 0 to A_y^0 such that the surface state quasienergy increases at a constant velocity $v = d\epsilon/dt$. As each crossing may be treated independently, the final probability to be in the surface state is just the product of the individual probabilities:

$$p_{ss}^A = \exp\left[-2\pi \sum_{j=1}^{N_c} \Delta_j^2/v\right] . \qquad (10)$$

This looks exactly like the L-Z problem for a single avoided crossing with matrix element $\Delta_{\text{eff}} = \sqrt{\sum_j \Delta_j^2}$, as illustrated in Fig. 4b. In the thermodynamic limit, we expect these gaps to scale as $\Delta_j \sim \Delta_0/\sqrt{L}$ from the scaling of the overlap of bulk and surface eigenstates. Thus the dynamics of our model is expected to have a consistent $L \to \infty$ limit, which is confirmed numerically in Fig. 3e. In addition to the final bulk occupation, this effective gap also controls the time scale of the oscillations in the surface state sidebands. Thus we see that both the incoherent transition to bulk states and coherent bulk-surface oscillations survive in the thermodynamic limit with dynamics set by the same emergent energy scale.

In addition to giving a physical picture for both the surface-bulk oscillations and the non-adiabatic tunneling of electrons into the bulk, the Demkov-Osherov model provides a handle for understanding how these should change with the various parameters, such as the experimentally-controllable τ_{pump}. One important upshot is the meaning of "adiabaticity" reversed from what we expect in the absence of resonances. Normally one expects the adiabatic limit to correspond to slow ramping, such that the system tracks the instantaneous Floquet eigenstate. However, it is clear for the resonant case that ramping the field too slowly will cause the entire population to transfer into the bulk. Therefore, to "adiabatically" track the surface state, one must instead use a fast ramp, though still sufficiently slow to prevent direct non-resonant excitations to the bulk.[73,75,81] More explicitly, we expect that the population remaining in the surface state at the end of the ramp should scale as $p_{ss}^f = e^{-4\pi\Delta_{\text{eff}}^2/v} \sim e^{-(4\pi\Delta_{\text{eff}}^2/\Delta\epsilon)\tau_{\text{pump}}} \equiv e^{-2\Gamma\tau_{\text{pump}}}$, where

the additional factor of two compared to Eq. 10 comes from ramping up to A_y^0 then back down to 0. This dependence is consistent with the data, as shown in Fig. 5d. By a similar token, increasing τ_{pump} increases the size of the resonant bulk-surface oscillations, as seen in Fig. 5a-c. It is interesting to note that a similar "ghost" surface state has been found in static models of topological materials coupled to a trivial bulk[82,83], which may be solved by modeling it with the well-known Fano model[84]. Ours is the natural Floquet generalization of these ideas, leading to fundamentally non-equilibrium phenomena such as coherent bulk-surface oscillations and Floquet resonances. Further discussion of the Demkov-Osherov model and its application to surface-driven systems may be found in Appendix B.

C. Applications to time-resolved ARPES

Before concluding this section, we note that our results our directly applicable to time-resolved ARPES experiments. Time-resolved pump-probe ARPES works by driving the system at frequency Ω with a Gaussian envelope (the pump) which excites that electrons in the sample but does not cause it to photoemit. Then, at variable times during the pump, a weak probe pulse at much higher frequency and much shorter width τ_{pr} is shone on the sample, which excites the driven electrons above the work function of the material. These electrons are then (photo)emitted by the sample and subsequently detected. By measuring the energy and momenta of the photoemitted electrons, the detector is able to map out the material's band structure during the probe pulse, including any non-equilibrium effects given by the pump.

Theoretically, the time-resolved ARPES signal for an arbitrary driven Hamiltonian $H(t)$ is given by[66,85]

$$I(\omega, t_{\text{av}}) = \text{Im}\left[\int dt_1 dt_2 s_{\text{pr}}(t_{\text{av}} - t_1) s_{\text{pr}}(t_{\text{av}} - t_2)\right.$$
$$\left. e^{i\omega(t_1 - t_2)} \text{Tr} G^< \left(t_1 - t_2, \frac{t_1 + t_2}{2}\right)\right] (11)$$

if one ignores that matrix elements between the electrons

in the material and the photoemitted states. A brief discussion of the effect of non-trivial matrix elements is found in Appendix C. If one uses a Gaussian probe, $s_{\text{pr}}(t) = \exp(-t^2/2\tau_{\text{pr}}^2)$, then Eq. 11 reduces to Eq. 9. Thus, all of the results we have shown so far can be simply interpreted as the signal of a time-resolved ARPES experiment with a Gaussian pump and probe, and our results serve as an important experimentally-accessible signature of this novel bulk-surface coupling.

III. LEADING CORRECTIONS IN FLOQUET ADIABATIC PERTURBATION THEORY

We have seen that, for slow pulses, non-adiabatic corrections to the Wigner distribution are dominated by resonances between the bulk and the surface. In this section, we will consider the other potential source of excitations, namely direct excitations to the bulk due to fast ramping of the drive. We will theoretically describe the leading corrections using Floquet adiabatic perturbation theory[81], placing the Wigner distribution on the same footing as static observables (cf.[75]). We will also use this to understand the *short* pump pulse limit, which remains relatively unexplored experimentally.

A. Basics of Floquet adiabatic perturbation theory (FAPT)

Adiabatic perturbation theory (APT) is a technique to derive leading corrections to the adiabatic limit for a system with a parameter λ that is ramped slowly with time[86–90]. Floquet APT (FAPT) extends this idea to a periodically driven system, which is relevant for our setup with parameter $\lambda = A_y$ ramped slowly during the pump pulse. Consider as before the case where the system starts with drive turned off in the single particle eigenstate $|0\rangle$ of undriven Hamiltonian $H(\lambda(t_0))$. Turning on the drive slowly, the full time evolution is captured in the wave function $|\psi(t)\rangle$. We can approximately solve the problem by doing a unitary rotation to the moving frame: $|\tilde{\psi}\rangle = V^\dagger|\psi\rangle$, where $V(\lambda(t), t) = P(\lambda, t)U_d(\lambda)$ is a unitary that maps the Floquet eigenstates $|n_F(\lambda, t)\rangle$ (see Eq. 6) to a fixed basis $|e_n\rangle$. In particular if we were to imagine turning on λ infinitely slowly in a gapped Floquet system, then the initial state $|0\rangle$ would just adiabatically track to the Floquet eigenstate $|\psi(t)\rangle = |0_F(\lambda, t)\rangle$ and $V^\dagger$ would act to map this to a time and λ-independent state $|\tilde{\psi}\rangle = |e_0\rangle$. For a generic time evolution $\lambda(t)$, the effective Hamiltonian in this moving frame is given by

$$H_m = U_d^\dagger H_F U_d - i\dot{\lambda}V^\dagger\partial_\lambda V \equiv H_F^d - \dot{\lambda}\tilde{A}_F, \qquad (12)$$

where H_F^d is a diagonal matrix whose entries correspond to the Floquet quasienenergies and $A_F(\lambda, t) = V\tilde{A}_F V^\dagger$ is the natural Floquet generalization of the Berry connection operator, with matrix elements

$\langle m_F(\lambda, t)|A_F|n_F(\lambda, t)\rangle = i\langle m_F(\lambda, t)|\partial_\lambda n_F(\lambda, t)\rangle$. In the adiabatic limit ($\dot{\lambda} \to 0$), off-diagonal elements of the second term in Eq. 12 are unable to cause transitions, which yields the adiabatic loading of the Floquet eigenstates as we just discussed.

Floquet APT consists of solving leading corrections to adiabaticity induced by the second term in Eq. 12. As this term is small due to the slow ramp rate $\dot{\lambda}$, it can be treated perturbatively. In particular, one may note that at fixed λ, $\tilde{A}_F$ is a periodic operator with Fourier series $\tilde{A}_F = \sum_\ell \tilde{A}_F^{(\ell)} e^{i\ell\Omega t}$ and similarly for V. Then Eq. 12 yields a Floquet problem which we can approximately solve using *static* perturbation theory. Expanding the wave function $|\psi(t)\rangle = \sum_n c_n |n_F(\lambda(t), t)\rangle$, the coefficients at leading order in adiabatic perturbation theory are given by[81]

$$c_0 \approx e^{-i\Theta_0(t)}$$

$$c_n \approx e^{-i\Theta_0(t)}\dot{\lambda}(t)\sum_\ell \frac{\langle e_n|\tilde{A}_F^{(\ell)}(\lambda(t))|e_0\rangle}{\epsilon_n^F(\lambda) - \epsilon_0^F(\lambda) + \ell\Omega}e^{i\ell\Omega t} . \quad (13)$$

The phase Θ_0 that the wave function picks up during the ramp consists of a dynamical and a Berry phase:

$$\Theta_0(t) = \int_{t_0}^t \left[\epsilon_0^F(\lambda(t')) - \dot{\lambda}(t')\langle e_0|\tilde{A}_F(\lambda(t'), t')|e_0\rangle\right]dt'.$$

This phase is usually neglected in most APT calculations of single-time observables, but is crucial to situations like ARPES where non-equilibrium observables are measured.

B. Application of FAPT to Wigner distribution

One can now use the approximate wave function $|\psi(t)\rangle$ derived above to obtain the Wigner distribution, $f(t_{\text{av}}, t_{\text{r}}) = \langle\psi(t_{\text{av}} + t_{\text{r}}/2)|\psi(t_{\text{av}} - t_{\text{r}}/2)\rangle$. For this Floquet problem, time enters in two ways: in the periodic part of the Floquet eigenstates, and in the slow time-dependence of λ. In the spirit of FAPT, we expand this slow dependence about the measurement point t_{av}, $\lambda(t_{\text{av}} \pm t_{\text{r}}/2) = \lambda(t_{\text{av}}) \pm t_{\text{r}}\dot{\lambda}(t_{\text{av}})/2 + O(\dot{\lambda}^2)$, and solve for the signal I keeping all terms to order $\dot{\lambda}$. This calculation is done in detail in Appendix D, with the following result:

$$I(\omega, t_{\text{pr}}) \approx \sum_\ell \left[(I_0^{(\ell)} + \Delta I^{(\ell)})e^{-[\omega - \omega_0^{(\ell)} - \Delta\omega^{(\ell)}]^2\tau_{\text{pr}}^2}\right] \quad (14)$$

$$\Delta\omega^{(\ell)} = \dot{\lambda}\left(\partial_\lambda\varphi^{(\ell)} - \sum_{\ell'} p_{0\ell'}\partial_\lambda\varphi^{(\ell')}\right)$$

$$\frac{\Delta I^{(\ell)}}{I_0^{(\ell)}} = \dot{\lambda}\sum_{n,\ell'}\left(\frac{\langle e_0|V^{(-\ell)\dagger}V^{(-\ell-\ell')}|e_n\rangle\langle e_n|\tilde{A}_F^{(\ell')}|e_0\rangle}{\epsilon_{n0}^F + \ell'\Omega}\right)$$

where all expressions are evaluate at time t_{pr}, the sum is taken for all pairs $(n, \ell') \neq (0, \ell)$, and notations are explained in the following paragraph.

The effects of these leading corrections to adiabaticity on the ARPES signal are illustrated in Fig. 6. Both the intensity $I_0^{(\ell)} = p_{0\ell} = \langle 0_F^{(\ell)} | 0_F^{(\ell)} \rangle$ and the frequency $\omega_0^{(\ell)} = \epsilon_0^F - \ell\Omega$ of the Floquet sideband $|0_F^{(\ell)}\rangle$ defined in Eq. 7 are modified by an amount proportional to the ramp rate $\dot{\lambda}$. The intensity shift $\Delta I^{(\ell)}$ results from virtual excitations of $|0_F^{(\ell')}\rangle$ to $|n_F^{(\ell+\ell')}\rangle$, which is a relatively standard prediction of adiabatic perturbation theory. Much more surprising are the frequency shifts, as they turn out to come from Berry phase effects. If we isolate the Berry phase sidebands as $|0_F^{(\ell)}\rangle = e^{i\varphi^{(\ell)}(\lambda)}|\tilde{0}_F^{(\ell)}(\lambda)\rangle$ such that $|\tilde{0}_F^{(\ell)}\rangle$ has vanishing Berry connection, then $\Delta\omega^{(\ell)}$ gives the difference of the Berry connection in sideband ℓ from the average Berry connection across all sidebands. This object seems somewhat bizarre if for no other reason than the fact that the Berry connection is not gauge-invariant. However, this difference of Berry connections *is* gauge invariant and leads to a Berry phase-dependent shift of the frequency of the sidebands.

Interestingly, while we think of adiabatic perturbation theory as primarily holding in the limit of small velocities, the results above actual hold in the limit of large (but not too large) velocities in which resonances can be neglected. Similar to the results found earlier in the resonant limit, these corrections in FAPT will lead to an asymmetry in the intensity signal with respect to time $t = 0$, even though the Gaussian pulse is symmetric with respect to $t = 0$. Unlike the resonant case, these corrections get smaller as the velocity decreases, or equivalently the pump time τ_{pump} increases, and the excitations that they describe are virtual, meaning that no real population will remain in the bulk. Combining this with our previous results, we see that as τ_{pump} is increased from zero, we get crossovers between various regimes, which are

1. $\tau_{\text{pump}} \ll 1/J, 1/\Delta$: Non-universal physics related to microscopic details.

2. $1/J, 1/\Delta \ll \tau_{\text{pump}} \ll 1/\Delta_{\text{res}}$: Virtual excitations described by Floquet adiabatic perturbation theory.

3. $1/\Delta_{\text{res}} \ll \tau_{\text{pump}}$: Real excitations due to surface-bulk resonances.

In the low-frequency weak-drive limit, we expect these regimes to be well separated[48], but whether such a separation of scales occurs in general is an important open question.

IV. DISCUSSION AND CONCLUSIONS

We have computed the Wigner distribution function for a driven topological insulator with bulk- surface coupling and study the effects of a pump pulse that weakly breaks the periodicity. If the drive is fixed, the Floquet states are well defined. However, the slow turn on and
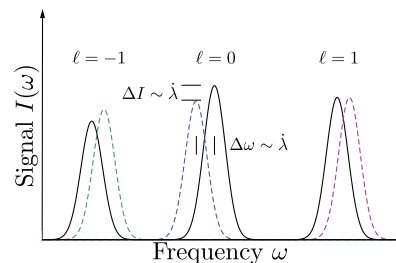

FIG. 6. Illustration of the effects of non-adiabaticity on the Floquet-ARPES signal with the FAPT approximation, leading to shifts in both the peak frequency and height proportional to the ramp rate $\dot{\lambda}$.

off of the drive breaks this periodicity and the Floquet states are no longer solutions of the Schrödinger equation. This leads to non-adiabatic population transfer from the surface states to the bulk. We track the origin to the existence of bulk-surface avoiding crossings in the the quasienergy spectrum, a signature of which are oscillations in the ARPES signal of a pump-probe type of experiment.

Finally we computed, using perturbation theory on the ramp rate of the drive amplitude, leading corrections to the "adiabatic" Floquet states. We showed that there are shifts of the resonances in the quasienergy spectrum. The shifts are a measure of the generalization of the Berry connection to periodically driven systems and can theoretically be seen in the ARPES spectrum.

These novel surface-bulk coupling effects are a very interesting paradigm to explore in future research. Many probes involve this basic setup, including ARPES, various types of scanning tip microscopy, photon-in photon-out scattering experiments, and many others. In systems with interesting topological surface states, or even traditional non-topological ones, this bulk/surface coupling upon resonant drive should yield interesting physically-measurable effects.

Topological insulators are rather weakly-correlated materials[91,92], so our treatment of them as non-interacting is well-justified. Generally, one expects this story to hold up against weak experimental realities such as interactions or disorder as long as the timescales associated with these processes are slower than those of the coherent bulk-surface oscillations. A more experimentally-relevant concern are phonons, which generally have a much stronger effect on bulk states than surface states[40]. This could have the potentially interesting effects of preferentially dephasing or relaxing higher harmonics of the surface states due to the presence of nearby in energy bulk states coupled by bulk phonons, while having a much weaker effect on surface harmonics that remain in the bulk gap. The effects of these experimentally-relevant factor remains an open topic for future research.

Finally, we note that driving the surface states of TIs and other materials was spurred by the search for novel

topological states[45–47] and rapidly expanded to other contexts[93–102]. In particular, it was proposed that driving a Dirac cone by circularly-polarized light could open a topological gap, yielding a Floquet Chern insulator. These proposals formally utilize the limit where Ω is much larger than the band gap, but experiments practically work in the opposite limit. The interesting open question is then what aspects of this topological character remain. There have been a number of recent studies that explored the interplay of bulk and surface states in systems driven at low frequencies[21,29,48,49], in which novel topological invariants were discovered that explicitly depend on the Floquet structure. However, those papers consider bulk driving of an initially trivial system, whereas our paper considers surface driving of an initially non-trivial system. We find seemingly unavoidable surface-bulk coupling which seems to close the Floquet gap and break down this topological classification for such driving. However, topological protection can also extend to gapless systems[13,103], so we leave the open question of how this surface driving affects the topological classification of the TI for future work.

[1] K. v. Klitzing, G. Dorda, and M. Pepper, Phys. Rev. Lett. **45**, 494 (1980).

[2] B. I. Halperin, Phys. Rev. B **25**, 2185 (1982).

[3] D. C. Tsui, H. L. Stormer, and A. C. Gossard, Phys. Rev. Lett. **48**, 1559 (1982).

[4] X.-G. WEN, *International Journal of Modern Physics B*, Int. J. Mod. Phys. B **06**, 1711 (1992).

[5] C. L. Kane and E. J. Mele, Phys. Rev. Lett. **95**, 146802 (2005).

[6] B. A. Bernevig, T. L. Hughes, and S.-C. Zhang, Science **314**, 1757 (2006).

[7] M. König, S. Wiedmann, C. Brüne, A. Roth, H. Buhmann, L. W. Molenkamp, X.-L. Qi, and S.-C. Zhang, Science **318**, 766 (2007).

[8] J. E. Moore and L. Balents, Phys. Rev. B **75**, 121306 (2007).

[9] L. Fu, C. L. Kane, and E. J. Mele, Phys. Rev. Lett. **98**, 106803 (2007).

[10] L. Fu and C. L. Kane, Phys. Rev. B **76**, 045302 (2007).

[11] D. Hsieh, D. Qian, L. Wray, Y. Xia, Y. S. Hor, R. J. Cava, and M. Z. Hasan, Nature **452**, 970 (2008).

[12] S. Murakami, New Journal of Physics **9**, 356 (2007).

[13] X. Wan, A. M. Turner, A. Vishwanath, and S. Y. Savrasov, Phys. Rev. B **83**, 205101 (2011).

[14] Z. K. Liu, B. Zhou, Y. Zhang, Z. J. Wang, H. M. Weng, D. Prabhakaran, S.-K. Mo, Z. X. Shen, Z. Fang, X. Dai, Z. Hussain, and Y. L. Chen, Science **343**, 864 (2014).

[15] S.-Y. Xu, C. Liu, S. K. Kushwaha, R. Sankar, J. W. Krizan, I. Belopolski, M. Neupane, G. Bian, N. Alidoust, T.-R. Chang, H.-T. Jeng, C.-Y. Huang, W.-F. Tsai, H. Lin, P. P. Shibayev, F.-C. Chou, R. J. Cava, and M. Z. Hasan, Science **347**, 294 (2015).

[16] S.-Y. Xu, I. Belopolski, N. Alidoust, M. Neupane, G. Bian, C. Zhang, R. Sankar, G. Chang, Z. Yuan, C.-C. Lee, S.-M. Huang, H. Zheng, J. Ma, D. S. Sanchez, B. Wang, A. Bansil, F. Chou, P. P. Shibayev, H. Lin, S. Jia, and M. Z. Hasan, Science **349**, 613 (2015).

[17] L. Lu, Z. Wang, D. Ye, L. Ran, L. Fu, J. D. Joannopoulos, and M. Soljačiċ, Science **349**, 622 (2015).

[18] A. Y. Kitaev, Physics-Uspekhi **44**, 131 (2001).

[19] J. E. Moore, Y. Ran, and X.-G. Wen, Phys. Rev. Lett. **101**, 186805 (2008).

[20] M. Levin and A. Stern, Phys. Rev. Lett. **103**, 196803 (2009).

[21] T. Kitagawa, E. Berg, M. Rudner, and E. Demler, Phys. Rev. B **82**, 235114 (2010).

[22] Y. Oreg, G. Refael, and F. von Oppen, Phys. Rev. Lett. **105**, 177002 (2010).

[23] R. M. Lutchyn, J. D. Sau, and S. Das Sarma, Phys. Rev. Lett. **105**, 077001 (2010).

[24] L. Fu, Phys. Rev. Lett. **106**, 106802 (2011).

[25] Y. Tanaka, Z. Ren, T. Sato, K. Nakayama, S. Souma, T. Takahashi, K. Segawa, and Y. Ando, Nat Phys **8**, 800 (2012).

[26] P. Dziawa, B. J. Kowalski, K. Dybko, R. Buczko, A. Szczerbakow, M. Szot, E. Lusakowska, T. Balasubramanian, B. M. Wojek, M. H. Berntsen, O. Tjernberg, and T. Story, Nat Mater **11**, 1023 (2012).

[27] V. Mourik, K. Zuo, S. M. Frolov, S. R. Plissard, E. P. A. M. Bakkers, and L. P. Kouwenhoven, Science **336**, 1003 (2012).

[28] Y. Okada, M. Serbyn, H. Lin, D. Walkup, W. Zhou, C. Dhital, M. Neupane, S. Xu, Y. J. Wang, R. Sankar, F. Chou, A. Bansil, M. Z. Hasan, S. D. Wilson, L. Fu, and V. Madhavan, Science **341**, 1496 (2013).

[29] P. Titum, E. Berg, M. S. Rudner, G. Refael, and N. H. Lindner, "The anomalous floquet-anderson insulator as a non-adiabatic quantized charge pump," ArXiv:1506.00650.

[30] J. Seo, P. Roushan, H. Beidenkopf, Y. S. Hor, R. J. Cava, and A. Yazdani, Nature **466**, 343 (2010).

[31] A. Gyenis, I. K. Drozdov, S. Nadj-Perge, O. B. Jeong, J. Seo, I. Pletikosi, T. Valla, G. D. Gu, and A. Yazdani, Phys. Rev. B **88**, 125414 (2013).

[32] S. Nadj-Perge, I. K. Drozdov, J. Li, H. Chen, S. Jeon, J. Seo, A. H. MacDonald, B. A. Bernevig, and A. Yazdani, Science **346**, 602 (2014).

[33] S. Jeon, B. B. Zhou, A. Gyenis, B. E. Feldman, I. Kimchi, A. C. Potter, Q. D. Gibson, R. J. Cava, A. Vishwanath, and A. Yazdani, Nat Mater **13**, 851 (2014).

[34] I. Zeljkovic, Y. Okada, M. Serbyn, R. Sankar, D. Walkup, W. Zhou, J. Liu, G. Chang, Y. J. Wang, M. Z. Hasan, F. Chou, H. Lin, A. Bansil, L. Fu, and V. Madhavan, Nat Mater **14**, 318 (2015).

[35] H. Inoue, A. Gyenis, Z. Wang, J. Li, S. W. Oh, S. Jiang, N. Ni, B. A. Bernevig, and A. Yazdani, Science **351**, 1184 (2016).

[36] W. H. Parker and W. D. Williams, Phys. Rev. Lett. **29**, 924 (1972).

[37] D. Hsieh, F. Mahmood, J. W. McIver, D. R. Gardner, Y. S. Lee, and N. Gedik, Phys. Rev. Lett. **107**, 077401 (2011).

[38] M. K. Liu, B. Pardo, J. Zhang, M. M. Qazilbash, S. J. Yun, Z. Fei, J.-H. Shin, H.-T. Kim, D. N. Basov, and R. D. Averitt, Phys. Rev. Lett. **107**, 066403 (2011).

[39] C. L. Smallwood, J. P. Hinton, C. Jozwiak, W. Zhang, J. D. Koralek, H. Eisaki, D.-H. Lee, J. Orenstein, and A. Lanzara, Science **336**, 1137 (2012).

[40] Y. H. Wang, D. Hsieh, E. J. Sie, H. Steinberg, D. R. Gardner, Y. S. Lee, P. Jarillo-Herrero, and N. Gedik, Phys. Rev. Lett. **109**, 127401 (2012).

[41] Y. H. Wang, H. Steinberg, P. Jarillo-Herrero, and N. Gedik, Science **342**, 453 (2013).

[42] W. Hu, S. Kaiser, D. Nicoletti, C. R. Hunt, I. Gierz, M. C. Hoffmann, M. Le Tacon, T. Loew, B. Keimer, and A. Cavalleri, Nat Mater **13**, 705 (2014).

[43] S. Kaiser, C. R. Hunt, D. Nicoletti, W. Hu, I. Gierz, H. Y. Liu, M. Le Tacon, T. Loew, D. Haug, B. Keimer, and A. Cavalleri, Phys. Rev. B **89**, 184516 (2014).

[44] M. Neupane, S.-Y. Xu, Y. Ishida, S. Jia, B. M. Fregoso, C. Liu, I. Belopolski, G. Bian, N. Alidoust, T. Durakiewicz, V. Galitski, S. Shin, R. J. Cava, and M. Z. Hasan, Phys. Rev. Lett. **115**, 116801 (2015).

[45] T. Oka and H. Aoki, Phys. Rev. B **79**, 081406 (2009).

[46] N. H. Lindner, G. Refael, and V. Galitski, Nat Phys **7**, 490 (2011).

[47] T. Kitagawa, T. Oka, A. Brataas, L. Fu, and E. Demler, Phys. Rev. B **84**, 235108 (2011).

[48] M. S. Rudner, N. H. Lindner, E. Berg, and M. Levin, Phys. Rev. X **3**, 031005 (2013).

[49] D. Carpentier, P. Delplace, M. Fruchart, and K. Gawedzki, Phys. Rev. Lett. **114**, 106806 (2015).

[50] R. Roy and F. Harper, "Abelian floquet spt phases in 1d," ArXiv:1602.08089 [cond-mat.str-el].

[51] A. C. Potter, T. Morimoto, and A. Vishwanath, "Topological classification of interacting 1d floquet phases," ArXiv:1602.05194 [cond-mat.str-el].

[52] C. W. von Keyserlingk and S. L. Sondhi, "Phase structure of 1d interacting floquet systems i: Abelian spts," ArXiv:1602.02157 [cond-mat.str-el].

[53] D. V. Else and C. Nayak, "On the classification of topological phases in periodically driven interacting systems," ArXiv:1602.04804 [cond-mat.str-el].

[54] X.-L. Qi, T. L. Hughes, and S.-C. Zhang, Phys. Rev. B **78**, 195424 (2008).

[55] A. M. Essin, J. E. Moore, and D. Vanderbilt, Phys. Rev. Lett. **102**, 146805 (2009).

[56] D. Hsieh, Y. Xia, D. Qian, L. Wray, J. H. Dil, F. Meier, J. Osterwalder, L. Patthey, J. G. Checkelsky, N. P. Ong, A. V. Fedorov, H. Lin, A. Bansil, D. Grauer, Y. S. Hor, R. J. Cava, and M. Z. Hasan, Nature **460**, 1101 (2009).

[57] S.-Y. Xu, Y. Xia, L. A. Wray, S. Jia, F. Meier, J. H. Dil, J. Osterwalder, B. Slomski, A. Bansil, H. Lin, R. J. Cava, and M. Z. Hasan, Science **332**, 560 (2011).

[58] C. Jozwiak, Y. L. Chen, A. V. Fedorov, J. G. Analytis, C. R. Rotundu, A. K. Schmid, J. D. Denlinger, Y.-D. Chuang, D.-H. Lee, I. R. Fisher, R. J. Birgeneau, Z.-X. Shen, Z. Hussain, and A. Lanzara, Phys. Rev. B **84**, 165113 (2011).

[59] B. M. Fregoso, Y. H. Wang, N. Gedik, and V. Galitski, Phys. Rev. B **88**, 155129 (2013).

[60] F. Mahmood, C.-K. Chan, Z. Alpichshev, D. Gardner, Y. Lee, P. A. Lee, and N. Gedik, Nat Phys **12**, 306 (2016).

[61] L. P. Kadanoff and G. Baym, *Quantum Statistical Mechanics* (Perseus Books, Cambridge, MA, 1989).

[62] M. Bukov and A. Polkovnikov, Phys. Rev. A **90**, 043613 (2014).

[63] H. Dehghani, T. Oka, and A. Mitra, Phys. Rev. B **90**, 195429 (2014).

[64] A. Farrell and T. Pereg-Barnea, "Dirac cones, floquet side bands and theory of time resolved arpes," ArXiv:1603.09718.

[65] S. V. Syzranov, M. V. Fistul, and K. B. Efetov, Phys. Rev. B **78**, 045407 (2008).

[66] M. Sentef, M. Claassen, A. Kemper, B. Moritz, T. Oka, J. Freericks, and T. Devereaux, Nat Commun **6**, 7047 (2015).

[67] More accurately, the electric field has this Gaussian envelope, but we can approximate this as just a Gaussian on $\mathbf{A}$ in the limit of a long pulse, $\tau_{\mathrm{pump}} \gg T$, which we consider throughout this paper.

[68] To get the "Floquet equilbrium" data shown in the figures for the bulk/surface coupled model, we have manually removed the resonances at each value of $\mathbf{k}$. This is accomplished by solving the Floquet problem exactly for a few different values of L between 85 and 115. Then we select the value of L for which the Floquet eigenstate has the most weight near the surface (i.e., for which $\langle z \rangle$ is minimized). Each L has a slightly different value of the resonances, so we are able to roughly get a smooth interpolations of the data "without resonances." This interpolating curve between the many values of L is picked out by eye and then fitted with a fifth-order polynomial.

[69] In practice, we actually just compute time evolution of the surface states on the upper surface as the remaining states do not affect the signal. We have verified that occupying the valence bands does not change our results.

[70] H. Weyl, Math. Ann. **77**, 313 (1916).

[71] J. S. Howland, Ann. Inst. Henri Poincaré Phys. Theor. **49**, 309 (1989).

[72] J. S. Howland, Ann. Inst. Henri Poincaré Phys. Theor. **49**, 325 (1989).

[73] D. W. Hone, R. Ketzmerick, and W. Kohn, Phys. Rev. A **56**, 4045 (1997).

[74] M. Bukov, M. Heyl, D. A. Huse, and A. Polkovnikov, Phys. Rev. B **93**, 155132 (2016).

[75] P. Weinberg, M. Bukov, L. D'Alessio, A. Polkovnikov, S. Vajna, and M. Kolodrubetz, "Adiabatic perturbation theory and geometry of periodically-driven systems," ArXiv:1606.02229.

[76] Y. N. Demkov and V. Osherov, Sov. Phys. JETP **26**, 916 (1968).

[77] J. H. Macek and M. J. Cavagnero, Phys. Rev. A **58**, 348 (1998).

[78] N. A. Sinitsyn, Phys. Rev. B **66**, 205303 (2002).

[79] L. Landau, Physics of the Soviet Union **2**, 46 (1932).

[80] C. Zener, Proceedings of the Royal Society of London A **137**, 696 (1932).

[81] K. Drese and M. Holthaus, The European Physical Journal D - Atomic, Molecular, Optical and Plasma Physics **5**, 119 (1999).

[82] D. L. Bergman and G. Refael, Phys. Rev. B **82**, 195417 (2010).

[83] Y. Baum, T. Posske, I. C. Fulga, B. Trauzettel, and A. Stern, Phys. Rev. Lett. **114**, 136801 (2015).

[84] U. Fano, Phys. Rev. **124**, 1866 (1961).

[85] J. K. Freericks, H. R. Krishnamurthy, and T. Pruschke, Phys. Rev. Lett. **102**, 136401 (2009).

[86] M. Born and V. Fock, Zeitschrift fÃŒr Physik **51**, 165 (1928).

[87] T. Kato, *Journal of the Physical Society of Japan*, J. Phys. Soc. Jpn. **5**, 435 (1950).

[88] S. Teufel, *Adiabatic perturbation theory in quantum dynamics* (Springer Science & Business Media, 2003).

[89] G. Rigolin, G. Ortiz, and V. H. Ponce, Phys. Rev. A **78**, 052508 (2008).

[90] C. De Grandi and A. Polkovnikov, *Quantum Quenching, Annealing and Computation*, edited by A. K. Chandra, A. Das, and B. Chakrabarti, Vol. 802 (Springer, 2010) pp. 75–114.

[91] Y. Xia, D. Qian, D. Hsieh, L. Wray, A. Pal, H. Lin, A. Bansil, D. Grauer, Y. S. Hor, R. J. Cava, and M. Z. Hasan, Nat Phys **5**, 398 (2009).

[92] D. Hsieh, Y. Xia, D. Qian, L. Wray, F. Meier, J. H. Dil, J. Osterwalder, L. Patthey, A. V. Fedorov, H. Lin, A. Bansil, D. Grauer, Y. S. Hor, R. J. Cava, and M. Z. Hasan, Phys. Rev. Lett. **103**, 146401 (2009).

[93] A. G. Grushin, A. Gómez-León, and T. Neupert, Phys. Rev. Lett. **112**, 156801 (2014).

[94] C.-K. Chan, P. A. Lee, K. S. Burch, J. H. Han, and Y. Ran, Phys. Rev. Lett. **116**, 026805 (2016).

[95] M. Fruchart, P. Delplace, J. Weston, X. Waintal, and D. Carpentier, Physica E: Low-dimensional Systems and Nanostructures **75**, 287 (2016).

[96] A. Quelle and C. Morais Smith, Phys. Rev. B **90**, 195137 (2014).

[97] S. Choudhury and E. J. Mueller, Phys. Rev. A **90**, 013621 (2014).

[98] J. P. Dahlhaus, B. M. Fregoso, and J. E. Moore, Phys. Rev. Lett. **114**, 246802 (2015).

[99] P. M. Perez-Piskunow, L. E. F. Foa Torres, and G. Usaj, Phys. Rev. A **91**, 043625 (2015).

[100] P. D. Sacramento, Phys. Rev. B **91**, 214518 (2015).

[101] D. E. Liu, Phys. Rev. B **91**, 144301 (2015).

[102] L. Privitera and G. E. Santoro, "Quantum annealing and non-equilibrium dynamics of floquet chern insulators," ArXiv:1508.01883 [quant-ph].

[103] S. Matsuura, P.-Y. Chang, A. P. Schnyder, and S. Ryu, New Journal of Physics **15**, 065001 (2013).

Appendix A: Further details of boundary-driven bulk TI model

In this appendix we briefly provide a more concrete definition of the Hamiltonian described the main text. As mentioned earlier, $k_{x,y}$ are conserved quantities, while k_z-dispersion becomes hopping. Labeling the sites along the z-direction as $j = 0, 1, \ldots, L-1$, the Hamiltonian may then be written

$$H = J \begin{pmatrix} H_{\mathrm{d}}^0 & H_{\mathrm{od}} & & \\ H_{\mathrm{od}}^\dagger & H_{\mathrm{d}}^1 & H_{\mathrm{od}} & \\ & H_{\mathrm{od}}^\dagger & \ddots & \\ & & & H_d^{L-1} \end{pmatrix},$$

$$H_{\mathrm{d}}^j = \tau^z \left[\sigma^x \sin(k_x + a_x^j) + \sigma^y \sin(k_y + a_y^j) \right] + \tau^x \left[m + 3 - \cos(k_x + a_x^j) - \cos(k_y + a_y^j) \right],$$

$$H_{\mathrm{od}} = \frac{i\sigma^z \tau^z - \tau^x}{2},$$

where the position-dependent vector potentials are $a_x^j = A_x \sin(\Omega t) \exp(-j/\xi)$ and $a_y^j = A_y \cos(\Omega t) \exp(-j/\xi)$. As noted in the main text, we work in the case $A_x = 0$ and $k_y = 0$ for all of the data shown.

Appendix B: Further details of the Demkov-Osherov model

The Demkov-Osherov (D-O) model consists of N parallel levels traversed by a single mode whose energy changes linearly with some parameter λ[76–78]. It can formally be solved when treated as a scattering problem, i.e., starting with some probability p_n^i in the states at $\lambda(t = -\infty) = -\infty$, λ is ramped linearly according to $\lambda = vt$ and the final probabilities at $t = \infty$ are obtained. The nice property of this model is that the level-crossings factorize, in the sense that the probability of ending up in one branch can be obtained by simply taking the semi-classical product of all the prior two-level (Landau-Zener) avoided crossings. Essentially this implies that in the long-time limit there are no interference effects between the various avoided crossings.

Motivated by the surface-bulk resonance discussed in Sec. II B, we will consider a particular subclass of D-O model illustrated in Fig. 7a. A total of L levels representing the bulk bands span the energy window $\epsilon_{\mathrm{bulk}} \in (-1/2, 1/2)$ while the surface state disperses with bare energy $\epsilon_0 = \lambda$ with some generic parameter λ taking the place of A_y. Gaps of strength $2\Delta_0/\sqrt{L}$ are opened uniformly between each bulk state and the surface state, which we will see gives a
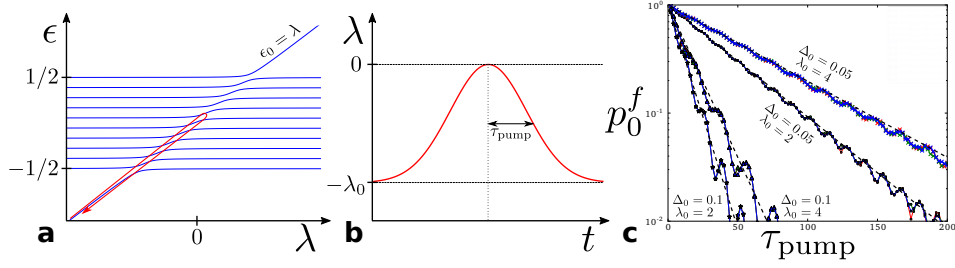
FIG. 7. Surface state occupation in Gaussian ramps of the Demkov-Osherov (D-O) model. (a) Illustration of the simplified D-O model that we consider (Eq. B1) with $L = 10$ levels. We simulate a Gaussian ramp to the middle of the bulk spectrum (b) and track the final surface state occupation $p_0^f = |\langle 0|\psi(t = \infty)\rangle|^2$ as function of the ramp rate τ_{pump} (c). The dashed lines show the predicted value $p_0^f = e^{-2\Gamma\tau_{\text{pump}}}$ with Γ from Eq. B3 showing a good fit for a variety of Δ_0 and λ_0.

well-defined thermodynamic limit. Choosing all matrix elements to be real and labeling the bulk states $|j = 1, \cdots, L\rangle$ and the surface state $|0\rangle$, this is described by the Hamiltonian

$$H = \lambda|0\rangle\langle 0| + \sum_{j=1}^{L} \epsilon_j|j\rangle\langle j| + \frac{\Delta_0}{\sqrt{L}} \sum_{j=1}^{L} (|0\rangle\langle j| + |j\rangle\langle 0|), \tag{B1}$$

where $\epsilon_j = (j - 1/2)/L - 1/2$.

We will be particularly interested in taking this model to the thermodynamic limit $L \to \infty$ and ascertaining what universal properties can be found in its dynamics. Consider first the exactly-solvable case where we start in the ground state $|0\rangle$ at $\lambda = -\infty$ and ramp linearly via $\lambda = vt$. Due to the fact that the crossings can be treated independently, at time $t = \infty$ the probability to remain in the surface state is simply $p_0^f = \prod_j e^{-2\pi\Delta_j^2/v} = e^{-2\pi\Delta_0^2/v}$, where $\Delta_j = \Delta_0/\sqrt{L}$ is the off-diagonal matrix element between $|0\rangle$ and $|j\rangle$. Note that this transition probability is identical to that of a single Landau-Zener transition with matrix element $\Delta_{\text{eff}} = \Delta_0$. While this effective gap only formally gives the final transition amplitude, one can readily confirm numerically that the dynamics of the occupation $p_0(t) = |\langle 0|\psi(t)\rangle|^2$ during the ramp is also well-approximated by that of a single avoided crossing of strength Δ_{eff}.

Let us now apply this intuitive approximation to arbitrary ramps $\lambda(t/\tau_{\text{pump}})$ set by some timescale τ_{pump} (e.g., the width of a Gaussian). A natural estimate for the transition probabilities is that they will again factorize but now with $v \to |v_j| = |\dot{\epsilon}_0(t_j)|$, where t_j is the time where the jth level is crossed: $\epsilon_0(\lambda(t_j)) = \epsilon_j$. Then if we start in the state $|0\rangle$ at time t_i and monotonically increase λ up to time t_f, such that $|v_j| = v_j$, the amount remaining in the surface state will be $p_0^{t_i \to t_f} \approx e^{-\alpha(t_i \to t_f)}$, where

$$\alpha(t_i \to t_f) = 2\pi \sum_i \Delta_i^2/v_i \overset{L\to\infty}{\to} 2\pi \int d\epsilon\, \nu(\epsilon) \frac{\Delta^2(\epsilon)}{d\epsilon/dt} = 2\pi\Delta_0^2 \int_{t_1}^{t_f} dt = 2\pi\Delta_0^2|z_1|\tau_{\text{pump}}, \tag{B2}$$

$\nu(\epsilon) = L$ is the density of bulk states, and $t_1(\lambda_i, \lambda_f) = z_1(\lambda_i, \lambda_f)\tau_{\text{pump}}$ is the time where the surface state first passes into the bulk, i.e., where it crosses ϵ_1. Note that this can be written as $p_0^{t_i \to t_f} \approx e^{-\Gamma\tau_{\text{pump}}}$ which looks like a constant rate Γ of surface states leaking into the bulk during the ramp.

The story becomes even more subtle if $\lambda(t)$ is not monotonic. Then the surface state may cross a given bulk state multiple times, and population that had transferred into the bulk may now return to the surface. However, we are already ignoring interference effects in the above model by, for instance, not ramping all the way to $\lambda = \infty$ to dephase the excitations. Therefore, at a similar level of approximation we may assume that no population, once transferred to the bulk, is able to return to the surface. Furthermore, if $\lambda(t)$ is an even function of time, then the magnitude of the velocity v_j for passing bulk level j during the first half of the ramp will be the same as during the second half of the ramp. Thus, we estimate the final surface occupation to be $p_0^f = e^{-2\Gamma\tau_{\text{pump}}}$, where Γ is given by Eq. B2. We numerically test this approximation using a Gaussian ramp that starts from $\lambda = -\lambda_0$ and ramps to $\lambda = 0$ as illustrated in Fig. 7b. Plugging this ramp profile into Eq. B2, we find

$$\Gamma_{\text{Gaussian}} = 2\pi\Delta_0^2\sqrt{-2\ln(1 - 1/(2\lambda_0))}. \tag{B3}$$

This estimate is plotted against exact simulation in Fig. 7c, showing a good fit. This justifies our independent-level Demkov-Osherov approximation for Gaussian ramps, which is used in the main text to fit the data in Fig. 5.
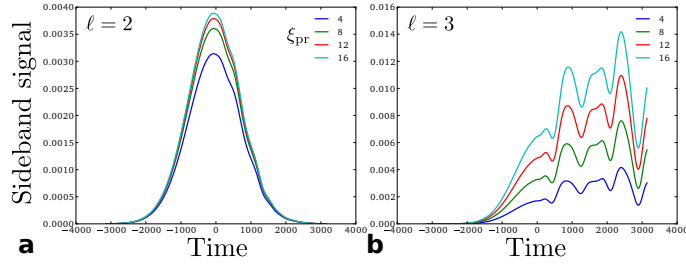
FIG. 8. Signal in the $\ell = 2$ and 3 sidebands as a function of the length scale ξ_{pr} for approximate ARPES matrix elements (Eq. C) using the same parameters as Fig. 3b. Data in previous figures is essentially the $\xi_{\mathrm{pr}} \to \infty$ limit of this model.

Appendix C: Matrix elements in ARPES

An additional complication in interpreting ARPES experiments is the fact that not all electrons photoemit with identical matrix elements, as we have tacitly assumed throughout this work. The general expression for the ARPES signal in the presence of photoemission matrix elements is significantly more complicated[85] and does not provide much insight to our analysis. However, we can slightly improve our approximation by simply weighting the states in $G^<$ by their position along the z-direction. The intuition behind this is that both the probe photons and the ionized electrons have some finite penetration depth or mean free path in the bulk before they are dissipated. Approximating this by a single length scale ξ_{pr}, we can introduce a weighting operator

$$\hat{W}_{\mathbf{k}_\parallel} = \sum_{j\alpha} e^{-j/\xi_{\mathrm{pr}}} |j\alpha\mathbf{k}_\parallel\rangle\langle j\alpha\mathbf{k}_\parallel|,$$

where $j = 0, 1, \ldots, L-1$ is the site number along the z-direction, $\alpha = 1 - 4$ are indices in the spin-orbital basis of σ and τ, and $\mathbf{k}_\parallel$ is the xy momentum as before. This operator just weights single-particle states by their position along z and thus we approximate the surface-weighted ARPES response by replacing f by

$$f'_n(t_{\mathrm{r}}, t_{\mathrm{av}}) = \langle\psi_n(t_{\mathrm{av}} + t_{\mathrm{r}}/2)|\hat{W}|\psi_n(t_{\mathrm{av}} - t_{\mathrm{r}}/2)\rangle.$$

The result with this surface projection are shown in Fig. 8 and allow us to compare surface and bulk behavior, particularly in higher Floquet sidebands. We see that the $\ell = 2$ sideband does not change significantly in either amplitude or character as ξ_{pr} is varied, which is consistent with its nature as a surface state. On the other hand, the $\ell = 3$ sideband is dominated by excitations into the bulk, which shows up as a strong increase in the signal with ξ_{pr}. On top of these bulk excitations, one expects a surface sideband signal as well, which should not depend on ξ_{pr} in the $\xi_{\mathrm{pr}} \to \infty$ limit. In principle we should be able to use this idea to distinguish the surface and bulk signals. Unfortunately, we are currently unable to do so with our data due to finite size effects; we leave this distinction of surface and bulk signals in the sidebands as a subject for future work.

Appendix D: Further details of FAPT

In this appendix, we will derive Eq. 14 by using the approximate time-dependent wave function derived using FAPT (Eq. 13) to obtain the Wigner distribution:

$$f(t_{\mathrm{av}}, t_{\mathrm{r}}) = \langle\psi(t_{\mathrm{av}} + t_{\mathrm{r}}/2)|\psi(t_{\mathrm{av}} - t_{\mathrm{r}}/2)\rangle \equiv \langle\psi(t_+)|\psi(t_-)\rangle$$

$$\approx e^{-i(\Theta_0(t_-)-\Theta_0(t_+))} \Bigg[\langle 0_F(\lambda_+, t_+)|0_F(\lambda_-, t_-)\rangle +$$

$$\dot{\lambda}_- \sum_{n\neq 0, \ell} \frac{\langle e_n|\tilde{A}_F^{(\ell)}(\lambda_-)|e_0\rangle}{\epsilon_{n0}^F(\lambda_-) + \ell\Omega} e^{i\ell(\Omega t_- - \varphi_0)} \langle 0_F(\lambda_+, t_+)|n_F(\lambda_-, t_-)\rangle + (\lambda_+ \leftrightarrow \lambda_-) \Bigg], \tag{D1}$$

where $t_\pm \equiv t_{\mathrm{av}} \pm t_{\mathrm{r}}/2$ and $\lambda_\alpha \equiv \lambda(t_\alpha)$. As mentioned in the main text, time enters via both the periodic part of the Floquet eigenstates and the slow time-dependence of λ, and we will expand this slow dependence about the t_{av}: $\lambda(t_\pm) = \lambda(t_{\mathrm{av}}) \pm t_{\mathrm{r}}\dot{\lambda}(t_{\mathrm{av}})/2 + O(\dot{\lambda}^2)$.

Let us now evaluate the terms in Eq. D1 one-by-one. First, consider the phase factor $e^{i\delta\Theta_0}$ where

$$\delta\Theta_0 = \Theta_0(t_+) - \Theta_0(t_-) = \int_{t_-}^{t_+} \left(\epsilon_0^F(\lambda(t')) - \dot\lambda(t')\langle e_0|\tilde A_F(\lambda(t'),t')|e_0\rangle \right) dt' \; . \tag{D2}$$

At order $\dot\lambda$, the energy can be expanded around $\lambda_{\rm av}$ as $\epsilon_0^F(\lambda(t')) \approx \epsilon_0^F(\lambda_{\rm av}) + \dot\lambda_{\rm av}(t'-t_{\rm av})\partial_\lambda\epsilon_0^F(\lambda_{\rm av})$. The second term is odd about $t_{\rm av}$, so it integrates to zero. Meanwhile, it is useful to express $\tilde A_F$ and V in terms of Fourier modes:

$$V(\lambda,t) = \sum_\ell e^{i\ell(\Omega t - \varphi_0)} V^{(\ell)}(\lambda) \tag{D3}$$

$$\tilde A_F(\lambda,t) = i\sum_{\ell,\ell'} e^{-i\ell'(\Omega t-\varphi_0)}V^{(\ell')\dagger}\partial_\lambda V^{(\ell)}e^{i\ell(\Omega t-\varphi_0)} \tag{D4}$$

$$\implies \tilde A_F^{(\ell)} = i\sum_{\ell'} V^{(\ell')\dagger}\partial_\lambda V^{(\ell+\ell')} . \tag{D5}$$

Throughout this appendix, we explicitly write the driving phase φ_0 to facilitate averaging over it as in Eq. 8. Then, replacing $\lambda(t')$ by $\lambda_{\rm av}$ in the second term of Eq. D2 to leading order in $\dot\lambda$ we get

$$\int_{t_-}^{t_+}\langle e_0|\tilde A_F(\lambda_{\rm av},t')|e_0\rangle dt' = \sum_\ell \int_{t_-}^{t_+} e^{i\ell(\Omega t'-\varphi_0)}\langle e_0|A_F^{(\ell)}|e_0\rangle dt' \tag{D6}$$

$$= \sum_\ell \frac{\langle e_0|\tilde A_F^{(\ell)}|e_0\rangle}{i\ell\Omega}\left(e^{i\ell(\Omega t_+ - \varphi_0)} - e^{i\ell(\Omega t_- - \varphi_0)}\right) \tag{D7}$$

$$= \sum_\ell \frac{\langle e_0|\tilde A_F^{(\ell)}|e_0\rangle}{i\ell\Omega}e^{i\ell(\Omega t_{\rm av}-\varphi_0)}\left(e^{i\ell\Omega t_{\rm r}/2} - e^{-i\ell\Omega t_{\rm r}/2}\right) \equiv iB_1 \; . \tag{D8}$$

Unless explicitly stated otherwise, all terms in the above expression are now evaluated at $\lambda_{\rm av}$, which is a trick we will employ throughout. Putting these terms together,

$$e^{i\delta\Theta_0} \approx e^{i\epsilon_0^F t_{\rm r}}e^{-i\dot\lambda_{\rm av}(iB_1)} \approx e^{i\epsilon_0^F t_{\rm r}}\left(1 + \dot\lambda_{\rm av}B_1\right) \; . \tag{D9}$$

Note that this first term in this product gives the main peak center as ϵ_0^F, the Floquet quasi-energy, while the terms like $e^{i\ell\Omega t_{\rm r}/2}$ in B_1 give additional satellite peaks offset by half-integer multiples of Ω. Later averaging over the phase φ_0 will remove all but the integer multiples of this frequency.

Next, we Taylor expand the term that appears to be $O(\dot\lambda^0)$ in Eq. D1 about time $t_{\rm av}$:

$$|0_F(\lambda(t_-),t_-)\rangle \approx |0_F(\lambda_{\rm av},t_-)\rangle - \frac{t_{\rm r}}{2}\dot\lambda_{\rm av}\partial_\lambda|0_F(\lambda_{\rm av},t_-)\rangle \tag{D10}$$

and similarly for the bra. Thus,

$$\langle 0_F(\lambda_+,t_+)|0_F(\lambda_-,t_-)\rangle \approx \underbrace{\langle 0_F(\lambda_{\rm av},t_+)|0_F(\lambda_{\rm av},t_-)\rangle}_{A_0} + \underbrace{\frac{\dot\lambda_{\rm av}t_{\rm r}}{2}\left(\langle\partial_\lambda 0_F(\lambda_{\rm av},t_+)|0_F(\lambda_{\rm av},t_-)\rangle - \langle 0_F(\lambda_{\rm av},t_+)|\partial_\lambda 0_F(\lambda_{\rm av},t_-)\rangle\right)}_{\dot\lambda A_1} .$$
$$\tag{D11}$$

Now $|0_F(\lambda,t)\rangle = V(\lambda,t)|e_0\rangle$, so $\partial_\lambda|0_F\rangle = \partial_\lambda V|e_0\rangle$. Thus

$$A_1 = \frac{t_{\rm r}}{2}\left(\langle e_0|\partial_\lambda V^\dagger(t_+)V(t_-)|e_0\rangle - \langle e_0|V^\dagger(t_+)\partial_\lambda V(t_-)|e_0\rangle\right) \tag{D12}$$

$$= \frac{t_{\rm r}}{2}\sum_{\ell',\ell''}\left(\langle e_0|\partial_\lambda V^{(\ell')\dagger}e^{-i\ell'(\Omega t_+-\varphi_0)}e^{i\ell''(\Omega t_- - \varphi_0)}V^{(\ell'')}|e_0\rangle - \langle e_0|V^{(\ell')\dagger}e^{-i\ell'(\Omega t_+-\varphi_0)}e^{i\ell''(\Omega t_--\varphi_0)}\partial_\lambda V^{(\ell'')}|e_0\rangle\right) \tag{D13}$$

$$= \frac{t_{\rm r}}{2}\sum_{\ell',\ell''}e^{-i(\ell'-\ell'')(\Omega t_{\rm av}-\varphi_0)}e^{-i(\ell''+\ell')\Omega t_{\rm r}/2}\left(\langle e_0|\partial_\lambda V^{(\ell')\dagger}V^{(\ell'')}|e_0\rangle - \langle e_0|V^{(\ell')\dagger}\partial_\lambda V^{(\ell'')}|e_0\rangle\right) . \tag{D14}$$

Meanwhile,

$$A_0 = \sum_{\ell',\ell''}e^{-i(\ell'-\ell'')(\Omega t_{\rm av}-\varphi_0)}e^{-i(\ell''+\ell')\Omega t_{\rm r}/2}\langle e_0|V^{(\ell')\dagger}V^{(\ell'')}|e_0\rangle \; . \tag{D15}$$

In the remaining two terms of Eq. D1, at order $\dot{\lambda}$ we can again replace $\lambda_{\pm}$ by λ_{av}. Then we can group these two terms into one that we denote $\dot{\lambda}_{\mathrm{av}}A_2$, with

$$A_2 = \sum_{n\neq 0,\ell}\left[\frac{\langle e_n|\tilde{A}_F^{(\ell)}|e_0\rangle}{\epsilon_{n0}^F+\ell\Omega}e^{i\ell(\Omega t_{\mathrm{av}}-\varphi_0)}e^{-i\ell\Omega t_{\mathrm{r}}/2}\langle 0_F(\lambda_{\mathrm{av}},t_+)|n_F(\lambda_{\mathrm{av}},t_-)\rangle+\right. \tag{D16}$$

$$\left.\frac{\langle e_0|\tilde{A}_F^{(\ell)\dagger}|e_n\rangle}{\epsilon_{n0}^F+\ell\Omega}e^{-i\ell(\Omega t_{\mathrm{av}})-\varphi_0}e^{-i\ell\Omega t_{\mathrm{r}}/2}\langle n_F(\lambda_{\mathrm{av}},t_+)|0_F(\lambda_{\mathrm{av}},t_-)\rangle\right]. \tag{D17}$$

Now

$$\langle 0_F(t_+)|n_F(t_-)\rangle = \langle e_0|V(t_+)^\dagger V(t_-)|e_n\rangle \tag{D18}$$

$$= \langle e_0|\left(\sum_{\ell',\ell''}V^{(\ell')\dagger}e^{-i\ell'(\Omega t_+-\varphi_0)}e^{i\ell''(\Omega t_--\varphi_0)}V^{(\ell'')}\right)|e_n\rangle \tag{D19}$$

$$= \langle e_0|\left(\sum_{\ell',\ell''}e^{i(\ell''-\ell')(\Omega t_{\mathrm{av}}-\varphi_0)}e^{-i(\ell''+\ell')\Omega t_{\mathrm{r}}/2}V^{(\ell')\dagger}V^{(\ell'')}\right)|e_n\rangle \tag{D20}$$

and similarly for $\langle n_F(t_+)|0_F(t_-)\rangle$. Thus

$$A_2 = \sum_{n\neq 0,\ell,\ell',\ell''}\left[\frac{\langle e_n|\tilde{A}_F^{(\ell)}|e_0\rangle\langle e_0|V^{(\ell')\dagger}V^{(\ell'')}|e_n\rangle}{\epsilon_{n0}^F+\ell\Omega}e^{i(\ell+\ell''-\ell')(\Omega t_{\mathrm{av}}-\varphi_0)}e^{-i(\ell+\ell'+\ell'')\Omega t_{\mathrm{r}}/2}+\right. \tag{D21}$$

$$\left.\frac{\langle e_0|\tilde{A}_F^{(\ell)\dagger}|e_n\rangle\langle e_n|V^{(\ell'')\dagger}V^{(\ell')}|e_0\rangle}{\epsilon_{n0}^F+\ell\Omega}e^{-i(\ell+\ell''-\ell')(\Omega t_{\mathrm{av}}-\varphi_0)}e^{-i(\ell+\ell'+\ell'')\Omega t_{\mathrm{r}}/2}\right]. \tag{D22}$$

Altogether,

$$f \approx e^{i\epsilon_0^F t_{\mathrm{r}}}(1+\dot{\lambda}_{\mathrm{av}}B_1)(A_0+\dot{\lambda}_{\mathrm{av}}A_1+\dot{\lambda}_{\mathrm{av}}A_2) \approx e^{i\epsilon_0^F t_{\mathrm{r}}}(A_0+\dot{\lambda}_{\mathrm{av}}\underbrace{(A_1+A_2+A_0B_1)}_{A_3})), \tag{D23}$$

where we can rewrite A_0B_1 as

$$A_0B_1 = \sum_{\ell,\ell',\ell''}\frac{\langle e_0|\tilde{A}_F^{(\ell)}|e_0\rangle\langle e_0|V^{(\ell')\dagger}V^{\ell''}|e_0\rangle}{\ell\Omega}e^{-i(\ell'-\ell''-\ell)(\Omega t_{\mathrm{av}}-\varphi_0)}e^{-i(\ell''+\ell')\Omega t_{\mathrm{r}}/2}\left(e^{-i\ell\Omega t_{\mathrm{r}}/2}-e^{i\ell\Omega t_{\mathrm{r}}/2}\right). \tag{D24}$$

Together with the expressions for $A_{0,1,2}$ above, this is the leading correction to $f(t_{\mathrm{av}},t_{\mathrm{r}})$. However, the observable ARPES signal comes from Fourier transforming this to get $f(t_{\mathrm{av}},\omega)$, then convolving in both the frequency and time direction by the Gaussian probe of width τ_{pr}, $e^{-\omega^2\tau_{\mathrm{pr}}^2}$ and $e^{-(t_{\mathrm{av}}-t_{\mathrm{pr}})^2/\tau_{\mathrm{pr}}^2}$ respectively, to get the ARPES signal $I(t_{\mathrm{pr}},\omega)$ at frequency ω for a probe centered at time t_{pr}. In the limit $\tau_{\mathrm{pr}}\gg T$ this convolution averages over many cycles as discussed earlier, which we treat by averaging over φ_0. Then, for instance, the "adiabatic" signal reduces to

$$\overline{A_0} = \sum_{\ell}\langle e_0|V^{(\ell)\dagger}V^{(\ell)}|e_0\rangle e^{-i\ell\Omega t_{\mathrm{r}}}, \tag{D25}$$

which yields the same Wigner distribution as Eq. 8.

Let's now calculate the leading correction, $\overline{A_3} = \overline{A_1}+\overline{A_2}+\overline{A_0B_1}$, term by term:

$$\overline{A_1} = \frac{t_{\mathrm{r}}}{2}\sum_{\ell}e^{-i\ell\Omega t_{\mathrm{r}}}\left[\langle e_0|\partial_\lambda V^{(\ell)\dagger}V^{(\ell)}|e_0\rangle-\langle e_0|V^{(\ell)\dagger}\partial_\lambda V^{(\ell)}|e_0\rangle\right] \tag{D26}$$

$$\overline{A_2} = \sum_{n\neq 0,\ell',\ell''}e^{-i\ell'\Omega t_{\mathrm{r}}}\left[\frac{\langle e_n|\tilde{A}_F^{(\ell'-\ell'')}|e_0\rangle\langle e_0|V^{(\ell')\dagger}V^{(\ell'')}|e_n\rangle}{\epsilon_{n0}^F+(\ell'-\ell'')\Omega}+h.c.\right] \tag{D27}$$

$$\overline{A_0B_1} = \sum_{\ell',\ell''}\frac{\langle e_0|\tilde{A}_F^{(\ell'-\ell'')}|e_0\rangle\langle e_0|V^{(\ell')\dagger}V^{(\ell'')}|e_0\rangle}{(\ell'-\ell'')\Omega}\left(e^{-i\ell'\Omega t_{\mathrm{r}}}-e^{-i\ell''\Omega t_{\mathrm{r}}}\right). \tag{D28}$$

It is worth noting that $\overline{A_0 B_1}$ naturally breaks up into "diagonal" and "off-diagonal" terms corresponding to $\ell' = \ell''$ and $\ell' \neq \ell''$ respectively. The diagonal term can be rewritten as

$$\left(\overline{A_0 B_1}\right)_d = \sum_{\ell' = \ell''} \frac{\langle e_0 | \tilde{A}_F^{(0)} | e_0 \rangle \langle e_0 | V^{(\ell')\dagger} V^{(\ell')} | e_0 \rangle}{(\ell' - \ell'')\Omega} e^{-i\ell'\Omega t_r} \left(1 - e^{-i(\ell'' - \ell')\Omega t_r} \right) \tag{D29}$$

$$= -i t_r \langle e_0 | \tilde{A}_F^{(0)} | e_0 \rangle \sum_{\ell'} \langle e_0 | V^{(\ell')\dagger} V^{(\ell')} | e_0 \rangle. \tag{D30}$$

This term along with $\overline{A_1}$ are the only ones proportional to t_r. They actually give rise to a shift of the peaks, since the Fourier transform of $it_r e^{iEt_r}$ is the derivative of the delta function, $\delta'(\omega - E)$. Combining these two terms gives

$$\overline{A_1} + \left(\overline{A_0 B_1}\right)_d = t_r \sum_\ell e^{-i\ell\Omega t_r} \left[\frac{\langle e_0 | \partial_\lambda V^{(\ell)\dagger} V^{(\ell)} | e_0 \rangle - h.c.}{2} - i \langle e_0 | \tilde{A}_F^{(0)} | e_0 \rangle \langle e_0 | V^{(\ell)\dagger} V^{(\ell)} | e_0 \rangle \right]. \tag{D31}$$

At this point it is useful to introduce the notation $|n_F^{(\ell)}\rangle = V^{(\ell)}|e_n\rangle$ as the ℓ-th Fourier mode of the n-th Floquet eigenstate as in Eq. 7. Then the first term in Eq. D31 looks like the Berry connection of $|0_F^{(\ell)}\rangle$ with the caveat that the state is not normalized. More explicitly, if we make so local gauge choice of states $|\tilde{0}_F^{(\ell)}(\lambda)\rangle$ such that their Berry connection is zero, i.e., $\langle \tilde{0}_F^{(\ell)}(\lambda) | \partial_\lambda \tilde{0}_F^{(\ell)}(\lambda) \rangle = 0$, then rewriting $|0_F^{(\ell)}\rangle = e^{i\varphi^{(\ell)}(\lambda)}|\tilde{0}_F^{(\ell)}\rangle$ we find $\langle 0_F^{(\ell)} | \partial_\lambda 0_F^{(\ell)} \rangle = i\partial_\lambda \varphi^{(\ell)} \langle 0_F^{(\ell)} | 0_F^{(\ell)} \rangle = i\partial_\lambda \varphi^{(\ell)} p_{0\ell}$. Factoring this out of each term in Eq. D31, we find

$$\overline{A_1} + \left(\overline{A_0 B_1}\right)_d = -i t_r \sum_\ell e^{-i\ell\Omega t_r} p_{0\ell} \left[\partial_\lambda \varphi^{(\ell)} - \sum_{\ell'} p_{0\ell'} \partial_\lambda \varphi^{(\ell')} \right]. \tag{D32}$$

In words the ℓ-th peak is shifted by an amount proportional to the difference between its Berry connection, $\partial_\lambda \varphi^{(\ell)}$, and the mode-averaged Berry connection, $\sum_{\ell'} p_0^{(\ell')} \partial_\lambda \varphi^{(\ell)}$. This is surprising, as the Berry connection is not gauge invariant and thus observables expressed in terms of it seem not gauge invariant on their face. However, the term above is in fact gauge invariant, which comes from the fact that all of the Fourier modes are shifted by the same the phase. To see this, consider a new gauge choice $|0'_F(\lambda, t)\rangle = e^{i\chi(\lambda)}|0_F(\lambda, t)\rangle$. Then

$$|0'_F(\lambda, t)\rangle = \sum_\ell e^{i\ell\Omega t}|0_F'^{(\ell)}\rangle = e^{i\chi(\lambda)} \sum_\ell e^{i\ell\Omega t}|0_F^{(\ell)}\rangle \implies |0_F'^{(\ell)}\rangle = e^{i\chi(\lambda)}|0_F^{(\ell)}\rangle. \tag{D33}$$

But then $\varphi^{(\ell)} \to \varphi^{(\ell)} + \chi$ and the χ contribution will clearly drop out in Eq. D32, since $\sum_{\ell'} p_{0\ell'} = 1$.

Meanwhile, the off-diagonal terms in $\overline{A_0 B_1}$ can be made to look more like $\overline{A_2}$. By first exchanging the indices ℓ' and ℓ'' in the second term followed by using the fact that $\tilde{A}_F^{(-\ell)} = \tilde{A}_F^{(\ell)\dagger}$ from the fact that $\tilde{A}_F(t)$ is Hermitian, we find that

$$\left(\overline{A_0 B_1}\right)_{od} = \sum_{\ell' \neq \ell''} \frac{\langle e_0 | \tilde{A}_F^{(\ell' - \ell'')} | e_0 \rangle \langle e_0 | V^{(\ell')\dagger} V^{(\ell'')} | e_0 \rangle}{(\ell' - \ell'')\Omega} \left(e^{-i\ell'\Omega t_r} - e^{-i\ell''\Omega t_r} \right) \tag{D34}$$

$$= \sum_{\ell' \neq \ell''} e^{-i\ell'\Omega t_r} \left(\frac{\langle e_0 | \tilde{A}_F^{(\ell' - \ell'')} | e_0 \rangle \langle e_0 | V^{(\ell')\dagger} V^{(\ell'')} | e_0 \rangle}{(\ell' - \ell'')\Omega} + h.c. \right) \tag{D35}$$

$$= \sum_{\ell'} e^{-i\ell'\Omega t_r} \sum_{\ell \neq 0} \left(\frac{\langle e_0 | \tilde{A}_F^{(\ell)} | e_0 \rangle \langle e_0 | V^{(\ell')\dagger} V^{(\ell' - \ell)} | e_0 \rangle}{\ell\Omega} + h.c. \right). \tag{D36}$$

Adding this to $\overline{A_2}$, we find that

$$\overline{A_2} + \left(\overline{A_0 B_1}\right)_{od} = \sum_{\ell'} e^{-i\ell'\Omega t_r} \sum_{(n,\ell) \neq (0,0)} \left(\frac{\langle e_0 | V^{(\ell')\dagger} V^{(\ell' - \ell)} | e_n \rangle \langle e_n | \tilde{A}_F^{(\ell)} | e_0 \rangle}{\epsilon_{n0}^F + \ell\Omega} + h.c. \right). \tag{D37}$$

It bears mentioning that the frequency shift is zero at this order in the undriven case. This can be seen from the above Floquet solution by replacing the quasienergies ϵ_n^F with the actual energies E_n and only allowing $\ell, \ell', \ell'' = 0$. Then the Berry connection term (Eq. D32) vanishes because one subtracts the Berry connection of the ground state

from itself. Similarly, the off-diagonal corrections (Eq. D37) vanish because the term $\langle e_0|V^{(0)\dagger}V^{(0)}|e_n\rangle = \langle E_0|E_n\rangle = 0$ from orthogonality of the energy eigenstates.

Finally, having solved for the Wigner distribution in terms of the average and relative times, we must Fourier transform and convolve with the probe to get the actual ARPES signal and see that there are no additional corrections to order $\dot{\lambda}$. We rewrite the diagonal (Eq. D32) and off-diagonal (Eq. D37) corrections as a_d and a_{od} respectively, such that

$$\overline{f}(t_r, t_{av}) \approx e^{i\epsilon_0^F t_r} \sum_\ell e^{-i\ell\Omega t_r} p_0^{(\ell)} \left[1 + \dot{\lambda}_{av}(a_{od}^{(\ell)} - it_r a_d^{(\ell)})\right]. \tag{D38}$$

This trivially Fourier transformed to get

$$\overline{f}(\omega, t_{av}) \approx 2\pi \sum_\ell p_0^{(\ell)} \left[(1 + \dot{\lambda}_{av} a_{od}^{(\ell)})\delta(\omega - \epsilon_0^F + \ell\Omega) + \dot{\lambda}_{av} a_d^{(\ell)} \delta'(\omega - \epsilon_0^F + \ell\Omega)\right]. \tag{D39}$$

Now let us convolve this Wigner distribution by a Gaussian probe to get the ARPES signal and confirm that these results are unaffected by smearing the δ-function peaks by Gaussians. First convolving along the ω direction (see Eq. 9), we get

$$
\begin{aligned}
I_1(\omega, t_{av}) &\equiv \int_{-\infty}^{\infty} d\omega' \overline{f}(\omega', t_{av}) e^{-(\omega'-\omega)^2 \tau_{pr}^2} \\
&\approx 2\pi \sum_\ell p_{0\ell} \big[(1 + \dot{\lambda}_{av} a_{od}^{(\ell)}) e^{-(\omega-\epsilon_0^F+\ell\Omega)^2 \tau_{pr}^2} \\
&\quad + 2\dot{\lambda}_{av} a_d^{(\ell)}(\omega - \epsilon_0^F + \ell\Omega)\tau_{pr}^2 e^{-(\omega-\epsilon_0^F+\ell\Omega)^2 \tau_{pr}^2}\big] \\
&\approx 2\pi \sum_\ell p_{0\ell} \left[(1 + \dot{\lambda}_{av} a_{od}^{(\ell)}) e^{-(\omega-\epsilon_0^F+\ell\Omega-\dot{\lambda}_{av} a_d^{(\ell)})^2 \tau_{pr}^2}\right],
\end{aligned}
$$

corresponding to a frequency shift of $\dot{\lambda}_{av} a_d^{(\ell)}$. Second, we must convolve in the time direction with the probe envelope $e^{-(t_{av}-t_{pr})^2/\tau_{pr}^2}$. The previous expression for $I_1(\omega, t_{av})$ only depends on t_{av} through λ_{av}. Therefore assuming that that probe is short such that λ does not significantly change during it (i.e., $\tau_{ramp} \gg \tau_{pr}$) we must ask when it is appropriate to simply replace t_{av} by t_{pr}. This clearly correct for all terms of order $\dot{\lambda}$, because doing a Taylor series in the difference $t_{av} - t_{pr}$ times the derivative of these terms with respect to λ would lead to corrections of order $\dot{\lambda}^2$. Thus the only potentially relevant correction comes from the term $p_{0\ell}(\lambda_{av}) \exp[-(\omega - \epsilon_0^F(\lambda_{av}) + \ell\Omega)] \equiv C_0(\lambda_{av})$. Fortunately, a Taylor expansion in $t_{av} - t_{pr}$ gives $\dot{\lambda}(t_{pr})(t_{av} - t_{pr})C_0'(\lambda_{pr})$, which is odd w.r.t. $(t_{av} - t_{pr})$ and thus vanishes under integration with the Gaussian. So at order $\dot{\lambda}$ we get our final answer for the ARPES signal:

$$I(\omega, t_{pr}) \approx \sum_\ell p_{0\ell} \left[(1 + \dot{\lambda}_{pr} a_{od}^{(\ell)}(\lambda_{pr})) e^{-[\omega-\epsilon_0^F(\lambda_{pr})+\ell\Omega-\dot{\lambda}_{pr} a_d^{(\ell)}(\lambda_{pr})]^2 \tau_{pr}^2}\right], \tag{D40}$$

which is the final result reproduced in Eq. 14.